

# Multimode Optomechanical Cooling via General Dark-Mode Control

Jian Huang,<sup>1</sup> Deng-Gao Lai,<sup>2</sup> Cheng Liu,<sup>1</sup> Jin-Feng Huang,<sup>1</sup> Franco Nori,<sup>2,3,4</sup> and Jie-Qiao Liao<sup>1,\*</sup>

<sup>1</sup>Key Laboratory of Low-Dimensional Quantum Structures and Quantum Control of Ministry of Education,  
Key Laboratory for Matter Microstructure and Function of Hunan Province,  
Department of Physics and Synergetic Innovation Center for Quantum Effects  
and Applications, Hunan Normal University, Changsha 410081, China

<sup>2</sup>Theoretical Quantum Physics Laboratory, RIKEN Cluster for Pioneering Research, Wako-shi, Saitama 351-0198, Japan

<sup>3</sup>RIKEN Center for Quantum Computing (RQC), 2-1 Hirosawa, Wako-shi, Saitama 351-0198, Japan

<sup>4</sup>Physics Department, The University of Michigan, Ann Arbor, Michigan 48109-1040, USA

(Dated: October 29, 2021)

The dark-mode effect is a stubborn obstacle for ground-state cooling of multiple degenerate mechanical modes optomechanically coupled to a common cavity-field mode. Here we propose an auxiliary-cavity-mode scheme for simultaneous ground-state cooling of two degenerate or near-degenerate mechanical modes by breaking the dark mode. We find that the introduction of the auxiliary cavity mode not only breaks the dark-mode effect, but also provides a new cooling channel to extract the thermal excitations stored in the dark mode. We also study the general physical-coupling configurations for breaking the dark mode in a generalized network-coupled four-mode optomechanical system consisting of two cavity modes and two mechanical modes. We derive the analytical dark-mode-breaking condition in this system. Our results not only provide a general method to control various dark-mode and dark-state effects in physics, but also pave the way to the study of macroscopic quantum phenomena and applications in multiple-mechanical-resonator systems.

PACS numbers:

**Introduction.**—Much recent interest in cavity optomechanics [1–3] has been paid to multimode optomechanical systems involving two [4–14] or multiple [15–25] mechanical resonators; and particularly the two-mechanical-mode optomechanical systems have been realized in several experimental platforms [7–14]. The study of multiple-mechanical-mode optomechanical systems has significance in both fundamental quantum physics [26] and modern quantum technologies [3]. For example, generation of macroscopic mechanical entanglement in multimode optomechanical systems has been experimentally demonstrated [10, 11, 13, 14]. Multimode optomechanical systems have also been considered to study quantum many-body effects [22–24], high performance sensors [27, 28], precise measurement [29], and nonreciprocal phonon or photon transport [30–37].

The simultaneous ground-state cooling of multiple mechanical modes has become a desired task because it is a prerequisite for the manipulation of macroscopic mechanical coherence [26]. Though great success has been made in cooling a single mechanical resonator in optomechanical systems [38–49], it remains a great challenge to perform ground-state cooling of multiple degenerate mechanical resonators coupled to a common cavity field, due to the mechanical dark-mode effect [7, 50–53]. For the two-mechanical-mode case, the dark-mode effect has been theoretically found [50] and experimentally demonstrated [53]. Meanwhile, the dark mode formed in optomechanical systems involving two cavity modes and one mechanical mode has also been found [54–57]. So far, theoretical proposals for optomechanical cooling of multiple mechanical resonators coupled in-series have been proposed [58, 59], and cooling of multimodes in a

resonator have been analyzed with the cold-damping feedback method [60, 61]. In addition, ground-state cooling of multiple mechanical resonators has been proposed based on synthetic magnetism [62] and reservoir engineering [63].

In this Letter, we propose an auxiliary-cavity-mode method for breaking the dark mode and further realizing ground-state cooling of two degenerate mechanical modes. We also explore the general coupling configurations for breaking the dark mode in a generalized four-mode optomechanical system, in which all the two-node couplings exist among two cavity modes and two mechanical modes. We find the analytical general conditions for forming and breaking the dark mode. Our results not only open up a new route to the realization of simultaneous ground-state cooling of two degenerate or near-degenerate mechanical resonators, but also initiate advances in dark-state engineering [64].

**System.**—Consider an “ $N$ ”-type four-mode optomechanical system consisting of two cavity modes (an intermediate cavity mode  $a$  and an auxiliary cavity mode  $a_s$ ) and two mechanical modes ( $b_1$  and  $b_2$ ), as shown in Fig. 1(a) when the couplings marked by the dashed lines are absent. The intermediate cavity mode is coupled to the two mechanical modes via radiation-pressure interactions. When the frequencies of the two mechanical modes are degenerate, a dark mode is formed in this linearized optomechanical system [40]. This dark mode decouples from the intermediate cavity mode, and hence the ground-state cooling of the two mechanical modes is largely suppressed. To break the dark-mode effect, we introduce the auxiliary cavity mode  $a_s$ , which is optomechanically coupled to the mechanical mode  $b_1$ . Moreover, two driving fields are applied to the cavity modes to control the optical

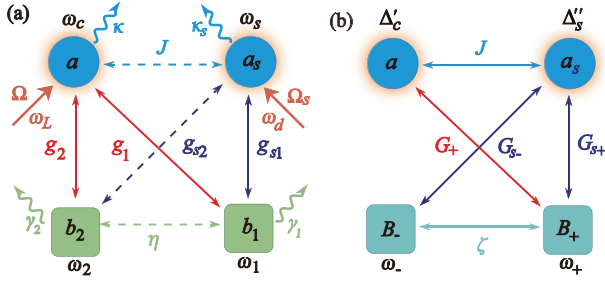


FIG. 1: (Color online) (a) Schematic of a network-coupled four-mode optomechanical system (reduced to the “N”-type coupled system when the three couplings marked by dashed lines are absent). (b) The coupling configuration associated with the linearized Hamiltonian (3).

and mechanical degrees of freedom. In a rotating frame defined by the operator  $\exp[-i(\omega_L a^\dagger a + \omega_d a_s^\dagger a_s)t]$ , the system Hamiltonian is given by ( $\hbar = 1$ )

$$H_I = \Delta_c a^\dagger a + \Delta_s a_s^\dagger a_s + \sum_{l=1,2} [\omega_l b_l^\dagger b_l + g_l a^\dagger a (b_l^\dagger + b_l)] + g_{s1} a_s^\dagger a_s (b_1^\dagger + b_1) + (\Omega a^\dagger + \Omega_s a_s^\dagger + \text{H.c.}), \quad (1)$$

where  $\Delta_c = \omega_c - \omega_L$  ( $\Delta_s = \omega_s - \omega_d$ ) is the driving detuning of the cavity frequency  $\omega_c$  ( $\omega_s$ ) with respect to its driving frequency  $\omega_L$  ( $\omega_d$ );  $a$  ( $a^\dagger$ ),  $a_s$  ( $a_s^\dagger$ ), and  $b_{l=1,2}$  ( $b_l^\dagger$ ) are, respectively, the annihilation (creation) operators of the intermediate cavity mode, the auxiliary cavity mode, and the  $l$ th mechanical mode, with the corresponding resonance frequencies  $\omega_c$ ,  $\omega_s$ , and  $\omega_l$ . The  $g_{l=1,2}$  ( $g_{s1}$ ) term in Eq. (1) describes the optomechanical coupling between the mechanical mode  $b_{l=1,2}$  ( $b_1$ ) and the cavity field  $a$  ( $a_s$ ). The parameters  $\omega_L$  ( $\omega_d$ ) and  $\Omega$  ( $\Omega_s$ ) are the driving frequency and amplitude associated with the driving field of the cavity mode  $a$  ( $a_s$ ), respectively.

**Ground-state cooling.**—We consider the strong-driving regime and then the system can be processed by the linearization procedure [65]. In this way, the operators  $o \in \{a, a^\dagger, a_s, a_s^\dagger, b_l, b_l^\dagger\}$  can be expressed as a sum of steady-state average values and quantum fluctuations, i.e.,  $o = \langle o \rangle_{ss} + \delta o$ . The linearized Langevin equations for these quantum fluctuations are given by  $\dot{\mathbf{u}}(t) = \mathbf{A}\mathbf{u}(t) + \mathbf{N}(t)$ , where  $\mathbf{u}(t) = [\delta a, \delta a_s, \delta b_1, \delta b_2, \delta a^\dagger, \delta a_s^\dagger, \delta b_1^\dagger, \delta b_2^\dagger]^T$  is the fluctuation operator vector with matrix transpose notation “ $T$ ”, and the coefficient matrix is defined by  $\mathbf{A} = \begin{pmatrix} \mathbf{E} & \mathbf{F} \\ \mathbf{F}^* & \mathbf{E}^* \end{pmatrix}$  with

$$\mathbf{E} = - \begin{pmatrix} \kappa + i\Delta'_c & 0 & iG_1 & iG_2 \\ 0 & \kappa_s + i\Delta'_s & iG_{s1} & 0 \\ iG_1^* & iG_{s1}^* & \gamma_1 + i\omega_1 & 0 \\ iG_2^* & 0 & 0 & \gamma_2 + i\omega_2 \end{pmatrix}, \quad (2)$$

and  $\mathbf{F}$  defined by these nonzero elements  $\mathbf{F}_{13} = -iG_1$ ,  $\mathbf{F}_{14} = -iG_2$ ,  $\mathbf{F}_{23} = -iG_{s1}$ ,  $\mathbf{F}_{31} = -iG_1$ ,  $\mathbf{F}_{32} = -iG_{s1}$ , and  $\mathbf{F}_{41} = -iG_2$ . Here  $\kappa$ ,  $\kappa_s$ , and  $\gamma_{l=1,2}$  are the decay rates of modes  $a$ ,  $a_s$ , and  $b_l$ , respectively. We also introduce the parameters  $\Delta'_c =$

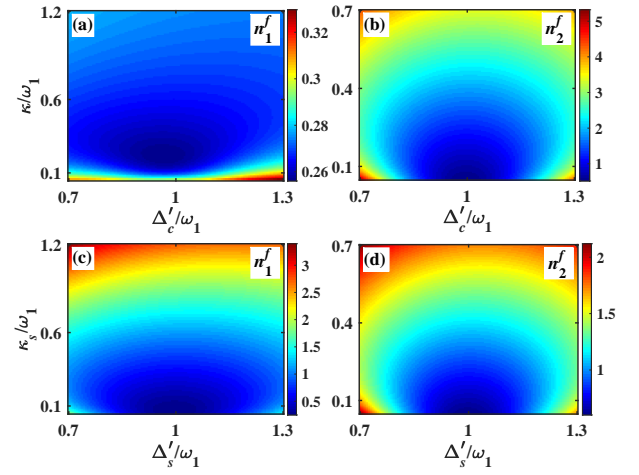


FIG. 2: (Color online) The final mean phonon numbers (a) [(c)]  $n_1^f$  and (b) [(d)]  $n_2^f$  of the two mechanical modes versus the scaled driving detuning  $\Delta'_c/\omega_1$  ( $\Delta'_s/\omega_1$ ) and the scaled cavity-field decay rate  $\kappa/\omega_1$  ( $\kappa_s/\omega_1$ ). Besides, the parameters  $\Delta'_s/\omega_1 = 1$  and  $\kappa_s/\omega_1 = 0.1$  are used in panels (a) and (b), the parameters  $\Delta'_c/\omega_1 = 1$  and  $\kappa/\omega_1 = 0.1$  are used in panels (c) and (d). Other parameters used are  $\omega_2/\omega_1 = 1$ ,  $\gamma_1/\omega_1 = \gamma_2/\omega_1 = 10^{-5}$ ,  $G_1/\omega_1 = G_2/\omega_1 = 0.05$ ,  $G_{s1}/\omega_1 = 0.08$ , and  $\bar{n}_1 = \bar{n}_2 = 1000$ .

$\Delta_c + 2g_1 \text{Re}[\beta_1] + 2g_2 \text{Re}[\beta_2]$  and  $\Delta'_s = \Delta_s + 2g_{s1} \text{Re}[\beta_1]$ , where  $\text{Re}[\beta_{l=1,2}]$  takes the real part of  $\beta_l$ .  $G_l = g_l \alpha$  ( $G_{s1} = g_{s1} \alpha_s$ ) is the linearized optomechanical-coupling strength between the cavity mode  $a$  ( $a_s$ ) and the mechanical mode  $b_l$  ( $b_1$ ). Here the steady-state displacements are determined by the relations  $\alpha \equiv \langle a \rangle_{ss} = -i\Omega/(\kappa + i\Delta'_c)$ ,  $\alpha_s \equiv \langle a_s \rangle_{ss} = -i\Omega_s/(\kappa_s + i\Delta'_s)$ ,  $\beta_1 \equiv \langle b_1 \rangle_{ss} = -i(g_1|\alpha|^2 + g_{s1}|\alpha_s|^2)/(\gamma_1 + i\omega_1)$ , and  $\beta_2 \equiv \langle b_2 \rangle_{ss} = -ig_2|\alpha|^2/(\gamma_2 + i\omega_2)$ . The eigensystem of the coefficient matrix  $\mathbf{A}$  determines the stability of the system, which can be obtained with the Routh-Hurwitz criterion [66]. In the following calculations, all the parameters used satisfy the stability conditions [65].

The noise operator vector in the Langevin equations is defined by  $\mathbf{N} = \sqrt{2}[\sqrt{\kappa}a_{\text{in}}, \sqrt{\kappa_s}a_{s,\text{in}}, \sqrt{\gamma_1}b_{1,\text{in}}, \sqrt{\gamma_2}b_{2,\text{in}}, \sqrt{\kappa}a_{\text{in}}^\dagger, \sqrt{\kappa_s}a_{s,\text{in}}^\dagger, \sqrt{\gamma_1}b_{1,\text{in}}^\dagger, \sqrt{\gamma_2}b_{2,\text{in}}^\dagger]^T$ , with  $a_{\text{in}}$  ( $a_{\text{in}}^\dagger$ ),  $a_{s,\text{in}}$  ( $a_{s,\text{in}}^\dagger$ ), and  $b_{l,\text{in}}$  ( $b_{l,\text{in}}^\dagger$ ) for  $l = 1, 2$  being the noise operators associated with modes  $a$ ,  $a_s$ , and  $b_l$ , respectively. These noise operators have zero mean values and obey the correlation functions [67, 68]:  $\langle a_{\text{in}}(t)a_{\text{in}}^\dagger(t') \rangle = \delta(t-t')$ ,  $\langle a_{\text{in}}^\dagger(t)a_{\text{in}}(t') \rangle = 0$ ,  $\langle a_{s,\text{in}}(t)a_{s,\text{in}}^\dagger(t') \rangle = \delta(t-t')$ ,  $\langle a_{s,\text{in}}^\dagger(t)a_{s,\text{in}}(t') \rangle = 0$ ,  $\langle b_{l,\text{in}}(t)b_{l,\text{in}}^\dagger(t') \rangle = (\bar{n}_l + 1)\delta(t-t')$ , and  $\langle b_{l,\text{in}}^\dagger(t)b_{l,\text{in}}(t') \rangle = \bar{n}_l\delta(t-t')$  for  $l = 1, 2$ , where  $\bar{n}_{l=1,2}$  is the average thermal-phonon occupation number associated with the  $l$ th mechanical mode.

The formal solution of the Langevin equations can be obtained as  $\mathbf{u}(t) = \mathbf{M}(t)\mathbf{u}(0) + \int_0^t \mathbf{M}(t-s)\mathbf{N}(s)ds$ , where we introduce the matrix  $\mathbf{M}(t) = \exp(\mathbf{A}t)$ . For cooling, we need to calculate the covariance matrix  $\mathbf{V}$  defined by  $V_{ij} = \frac{1}{2}[\langle \mathbf{u}_i(\infty)\mathbf{u}_j(\infty) \rangle + \langle \mathbf{u}_j(\infty)\mathbf{u}_i(\infty) \rangle]$  for  $i, j = 1-8$ . In this linearized optomechanical system, the covariance matrix  $\mathbf{V}$  satisfies the Lyapunov equation  $\mathbf{A}\mathbf{V} + \mathbf{V}\mathbf{A}^T = -\mathbf{Q}$  [69]. Here,

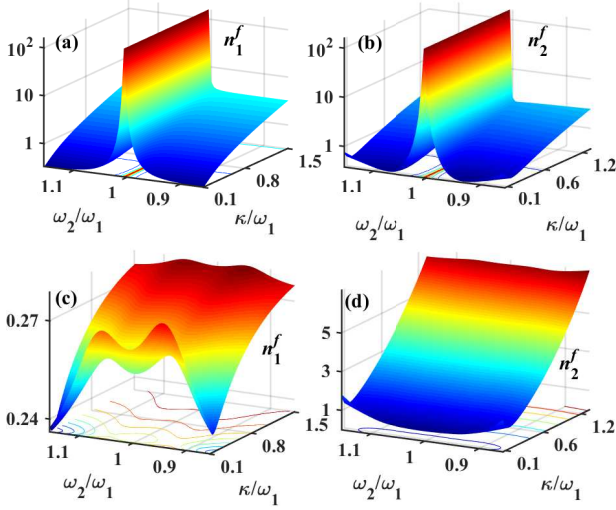


FIG. 3: (Color online) The final mean phonon numbers  $n_1^f$  and  $n_2^f$  versus the frequency ratio  $\omega_2/\omega_1$  and the scaled cavity-field decay rate  $\kappa/\omega_1$  in [(a) and (b)] the case of dark-mode-unbreaking ( $G_{s1}/\omega_1 = 0$ ) and [(c) and (d)] the case of dark-mode-breaking ( $G_{s1}/\omega_1 \neq 0$ ). Other parameters used are  $\Delta'_c = \Delta'_s = \omega_1$ ,  $\kappa_s/\omega_1 = 0.1$ ,  $G_1/\omega_1 = G_2/\omega_1 = 0.05$ ,  $G_{s1}/\omega_1 = 0.08$ ,  $\gamma_1/\omega_1 = \gamma_2/\omega_1 = 10^{-5}$ , and  $\bar{n}_1 = \bar{n}_2 = 1000$ .

the matrix  $\mathbf{Q}$  is defined by  $\mathbf{Q} = \frac{1}{2}(\mathbf{C} + \mathbf{C}^T)$ , where  $\mathbf{C}$  is the noise correlation matrix defined by  $\langle \mathbf{N}_k(s) \mathbf{N}_l(s') \rangle = \mathbf{C}_{k,l} \delta(s - s')$  for  $k, l = 1-8$ . For the Markovian dissipation,  $\mathbf{C}$  is obtained with the nonzero elements  $\mathbf{C}_{15} = 2\kappa$ ,  $\mathbf{C}_{26} = 2\kappa_s$ ,  $\mathbf{C}_{37} = 2\gamma_1(\bar{n}_1 + 1)$ ,  $\mathbf{C}_{48} = 2\gamma_2(\bar{n}_2 + 1)$ ,  $\mathbf{C}_{73} = 2\gamma_1\bar{n}_1$ , and  $\mathbf{C}_{84} = 2\gamma_2\bar{n}_2$ . By solving the Lyapunov equation, we obtain the covariance matrix  $\mathbf{V}$ , then the final mean phonon numbers of the two mechanical modes are given by  $n_1^f = \langle \delta b_1^\dagger \delta b_1 \rangle = \mathbf{V}_{73} - 1/2$  and  $n_2^f = \langle \delta b_2^\dagger \delta b_2 \rangle = \mathbf{V}_{84} - 1/2$ .

To exhibit the function of the auxiliary-cavity coupling on the cooling in the two-degenerate-mode case ( $\omega_1 = \omega_2$ ), in Fig. 2 we plot the final mean phonon numbers  $n_1^f$  and  $n_2^f$  as functions of the scaled driving detuning  $\Delta'_c/\omega_1$  ( $\Delta'_s/\omega_1$ ) and the scaled cavity-field decay rate  $\kappa/\omega_1$  ( $\kappa_s/\omega_1$ ). In Figs. 2(a) and 2(b), we can see that the ground-state cooling of the two mechanical modes can be realized in the resolved-sideband limit ( $\kappa/\omega_1 \ll 1$ ) and around the red-sideband resonance  $\Delta'_c/\omega_1 \sim 1$ . In Figs. 1(c) and 1(d), we see that the ground-state cooling of the two mechanical modes can be realized in the resolved-sideband limit ( $\kappa_s/\omega_1 \ll 1$ ), and that the cooling performance is best at the optimal driving detuning  $\Delta'_s/\omega_1 \approx 1$ .

Next we analyze the influence of the frequency mismatch between the two mechanical modes on the cooling efficiency, in Figs. 3(a) and 3(b) we plot the phonon numbers  $n_1^f$  and  $n_2^f$  versus the frequency ratio  $\omega_2/\omega_1$  and the scaled cavity-field decay rate  $\kappa/\omega_1$  in the absence of the auxiliary cavity mode ( $G_{s1}/\omega_1 = 0$ ). Here, we see that the final mean phonon numbers in the two mechanical modes cannot be efficiently decreased around  $\omega_2 = \omega_1$ , which means

that the two mechanical modes cannot be cooled to their ground states when their frequencies are degenerate or near-degenerate (in a finite-detuning window). This phenomenon can be explained according to the dark-mode effect. In the degenerate-resonator case ( $\omega_1 = \omega_2$ ), a bright mode and a dark mode are formed in this optomechanical system. Physically, the two mechanical modes have an obvious spectral overlap and become effectively degenerate in the presence of dissipation, thus the dark-mode effect works in the near-degenerate case. The dark mode decouples from both the cavity mode and the bright mode, so the phonon excitations stored in the dark mode cannot be extracted out through the optomechanical-cooling channel [62]. However, the dark-mode effect disappears when the two mechanical modes are far-off-resonant, thus achieving ground-state cooling. In Figs. 3(c) and 3(d), we plot the phonon numbers  $n_1^f$  and  $n_2^f$  versus the frequency ratio  $\omega_2/\omega_1$  and the scaled decay rate  $\kappa/\omega_1$ , when the auxiliary cavity field is present ( $G_{s1}/\omega_1 = 0.08$ ). Here the ground-state cooling of the two mechanical modes can be achieved ( $n_{1,2}^f \ll 1$ ) when the system works in the resolved-sideband regime ( $\kappa \ll \omega_1$ ). Here the first mechanical resonator has a better cooling efficiency ( $n_1^f < n_2^f$ ) because it is connected to two cooling channels at the same time.

*General dark-mode control.*—To find out a general dark-mode-breaking condition, we consider a generalized network-coupled four-mode optomechanical system including all the two-node couplings [Fig. 1(a) including the three dashed-line couplings]. In a rotating frame defined by the operator  $\exp[-i(\omega_L a^\dagger a + \omega_d a_s^\dagger a_s)t]$  under  $\omega_L = \omega_d$ , the Hamiltonian of the generalized system reads  $H_{\text{net}}^f = H_I + J(a^\dagger a_s + a_s^\dagger a) + \eta(b_1^\dagger b_2 + b_2^\dagger b_1) + g_{s2} a_s^\dagger a_s (b_2^\dagger + b_2)$ , where  $J$ ,  $\eta$ , and  $g_{s2}$  are the coupling strengths corresponding to the photon hopping, the phonon hopping, and the optomechanical interaction between modes  $a_s$  and  $b_2$ , respectively. To analyze the dark-mode effect in this system, we assume that the two coupling channels  $g_1$  and  $g_2$  always exist and the remaining couplings can be closed on demand. Depending on the existence of other coupling channels or not, there are fourteen cases of coupling configurations [65]. We follow the linearization procedure and perform the cooling calculations for these cases [65].

In Fig. 4 we show the final mean phonon numbers  $n_1^f$  and  $n_2^f$  as functions of the scaled decay rate  $\kappa/\omega_1$  in these fourteen cases. Figures 4(a) and 4(b) show that the ground-state cooling of the two mechanical resonators can (cannot) be realized in the cases of  $G_{s1} = 0$  or  $G_{s2} = 0$  ( $J = 0$  or  $\eta = 0$ ), which implies that the dark mode can (cannot) be broken. In Figs. 4(c) and 4(d), we plot the phonon numbers  $n_1^f$  and  $n_2^f$  versus  $\kappa/\omega_1$  when two of the four coupling channels ( $J$ ,  $G_{s1}$ ,  $G_{s2}$ , and  $\eta$ ) are closed. The cooling performance implies that the dark mode cannot be broken when the coupling channels  $J = \eta = 0$  or  $G_{s1} = G_{s2} = 0$ . In these four cases:  $J = G_{s1} = 0$ ,  $J = G_{s2} = 0$ ,  $\eta = G_{s1} = 0$ , and  $\eta = G_{s2} = 0$ , the dark mode can be broken. In Figs. 4(e) and 4(f), we display the cooling performance when three of the four coupling channels



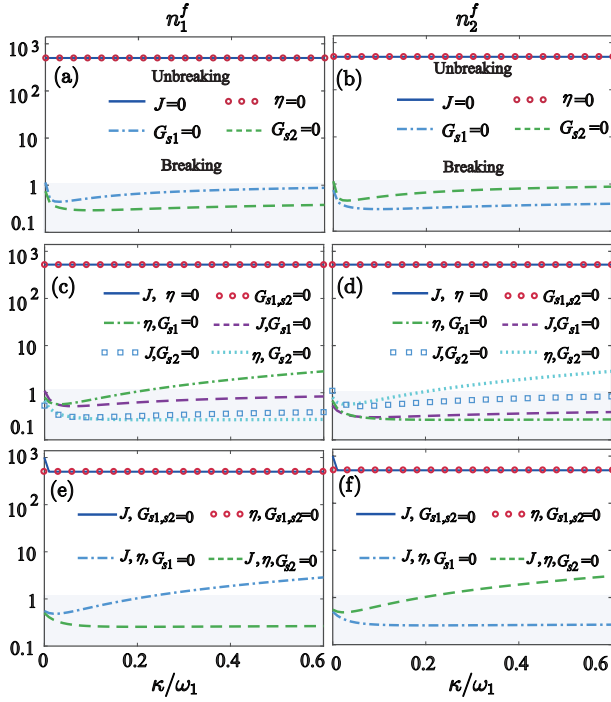


FIG. 4: (Color online) The final mean phonon numbers  $n_1^f$  and  $n_2^f$  versus  $\kappa/\omega_1$  for various coupling configurations (closed couplings are marked in panels). Other parameters are taken as  $\omega_2/\omega_1 = 1$ ,  $\gamma_1/\omega_1 = \gamma_2/\omega_1 = 10^{-5}$ ,  $\kappa/\omega_1 = \kappa_s/\omega_1 = 0.1$ ,  $J/\omega_1 = \eta/\omega_1 = 0.03$ ,  $\Delta'_c/\omega_1 = \Delta''_c/\omega_1 = 1$ ,  $G_1/\omega_1 = G_2/\omega_1 = 0.05$ ,  $G_{s1}/\omega_1 = G_{s2}/\omega_1 = 0.08$ , and  $\bar{n}_1 = \bar{n}_2 = 1000$ . Note that the values of  $J$ ,  $\eta$ ,  $G_{s1}$ , and  $G_{s2}$  presented here work when the corresponding coupling channels are open, and that the coupling strengths before and after the linearization are related by  $G_{l=1,2} = g_l \alpha$  and  $G_{s1} = g_{s1} \alpha_s$ .

are closed. Here, we see that the dark mode cannot be broken when  $J = G_{s1} = G_{s2} = 0$  or  $\eta = G_{s1} = G_{s2} = 0$ . However, in the two cases of  $J = \eta = G_{s1} = 0$  or  $J = \eta = G_{s2} = 0$ , the dark mode can be broken [65].

The dark-mode effect in the above cases can be clarified by analytically deriving the dark-mode-existing condition [65]. To this end, we derive an effective Hamiltonian which governs the linearized dynamics of the system as [see Fig. 1(b)]

$$H_{\text{RWA}} = \Delta'_c \delta a^\dagger \delta a + \Delta''_s \delta a_s^\dagger \delta a_s + J(\delta a^\dagger \delta a_s + \delta a_s^\dagger \delta a) + \omega_+ B_+^\dagger B_+ + \omega_- B_-^\dagger B_- + \zeta(B_+^\dagger B_- + B_-^\dagger B_+) + G_+(\delta a B_+^\dagger + B_+ \delta a^\dagger) + G_{s+}(\delta a_s B_+^\dagger + \delta a_s^\dagger B_+) + G_{s-}(\delta a_s B_-^\dagger + \delta a_s^\dagger B_-), \quad (3)$$

where we introduce two hybrid mechanical modes  $B_+ = (G_1 \delta b_1 + G_2 \delta b_2)/G_+$  and  $B_- = (G_2 \delta b_1 - G_1 \delta b_2)/G_+$ , with  $G_+ = (G_1^2 + G_2^2)^{1/2}$ . The parameters in Eq. (3) are given by  $\Delta'_s = \Delta_s + 2g_{s1} \text{Re}[\beta_1] + 2g_{s2} \text{Re}[\beta_2]$ ,  $\omega_+ = (\omega_1 G_1^2 + \omega_2 G_2^2 + 2\eta G_1 G_2)/G_+^2$ ,  $\omega_- = (\omega_1 G_2^2 + \omega_2 G_1^2 - 2\eta G_1 G_2)/G_+^2$ ,  $\zeta = [(\omega_1 - \omega_2)G_1 G_2 + \eta(G_2^2 - G_1^2)]/G_+^2$ ,  $G_{s+} = (G_{s1} G_1 + G_{s2} G_2)/G_+$  and  $G_{s-} = (G_{s1} G_2 - G_{s2} G_1)/G_+$ . Here these linearized optomechanical-coupling strengths have a similar definition as before, and the displacement amplitudes should be changed by including the new couplings [65]. We can see that the mode  $B_+$  always couples to the cavity field because of  $G_+ > 0$ , and

that the parameter conditions for the appearance of the dark mode (namely mode  $B_-$  decoupling from other three modes) are  $\zeta = 0$  and  $G_{s-} = 0$ , which lead to

$$(\omega_1 - \omega_2)G_1 G_2 + \eta(G_2^2 - G_1^2) = 0, \quad (4a)$$

$$G_{s1} G_2 - G_{s2} G_1 = 0. \quad (4b)$$

Therefore, the general dark-mode-breaking condition is that both  $\zeta$  and  $G_{s-}$  cannot be zero at the same time. Based on Eq. (4), the cooling performance in the above fourteen cases can be explained clearly [65].

Below we analyze the parameter conditions (4) in detail.

(i) Equation (4a) is determined by the parameters of the “ $\Lambda$ ”-type three-mode system involving modes  $a$ ,  $b_1$ , and  $b_2$ , and it gives the condition for forming a dark mode in the three-mode system: When  $\eta = 0$ , the dark mode appears at  $\omega_1 = \omega_2$ , irrespectively of the nonzero values of  $G_1$  and  $G_2$ ; When  $\eta \neq 0$  and  $\omega_1 = \omega_2$ , the dark mode exists only when  $G_1 = G_2$ . Meanwhile, Eq. (4b) introduces the auxiliary cavity mode. Mode  $B_-$  always couples to the system once  $G_{s1}/G_{s2} \neq G_1/G_2$ . (ii) In the degenerate-resonator case  $\omega_1 = \omega_2$ , the conditions (4) are reduced to  $\eta(G_2^2 - G_1^2) = 0$  and  $G_{s1} G_2 - G_{s2} G_1 = 0$ . The dark mode appears when both  $G_{s1}/G_{s2} = G_1/G_2$  and either one of the two relations  $\eta = 0$  and  $G_1 = G_2$  are satisfied. (iii) In the non-degenerate-resonator case  $\Delta\omega = \omega_1 - \omega_2 \neq 0$ , the dark mode appears only when  $\chi \equiv G_2/G_1 = \frac{1}{2}[-\Delta\omega/\eta \pm \sqrt{(\Delta\omega/\eta)^2 + 4}]$  and  $G_{s1}/G_{s2} = 1/\chi$ .

*Conclusion.*—We have proposed an auxiliary-cavity-mode method to realize simultaneous ground-state cooling of two degenerate or near-degenerate mechanical modes. We have also studied the general physical coupling configuration for breaking the dark mode in the network-coupled four-mode optomechanical system. The analytical parameter conditions for breaking the dark-mode effect have been found. Our results pave a way toward the demonstration of macroscopic quantum coherence and quantum manipulation in multiple-mechanical-mode optomechanical systems.

J.-Q.L. is supported in part by National Natural Science Foundation of China (Grants No. 11822501, No. 11774087, No. 12175061, and No. 11935006) and Hunan Science and Technology Plan Project (Grant No. 2017XK2018). J.-F.H. is supported in part by the National Natural Science Foundation of China (Grant No. 12075083), Scientific Research Fund of Hunan Provincial Education Department (Grant No. 18A007), and Natural Science Foundation of Hunan Province, China (Grant No. 2020JJ5345). F.N. is supported in part by: Nippon Telegraph and Telephone Corporation (NTT) Research, the Japan Science and Technology Agency (JST) [via the Quantum Leap Flagship Program (Q-LEAP), the Moonshot R&D Grant Number JPMJMS2061, and the Centers of Research Excellence in Science and Technology (CREST) Grant No. JPMJCR1676], the Japan Society for the Promotion of Science (JSPS) [via the Grants-in-Aid for Scientific Research (KAKENHI) Grant No. JP20H00134 and the JSPS-RFBR Grant No. JPJSBP120194828], the Army

Research Office (ARO) (Grant No. W911NF-18-1-0358), the Asian Office of Aerospace Research and Development (AOARD) (via Grant No. FA2386-20-1-4069), and the Foundational Questions Institute Fund (FQXi) via Grant No. FQXi-IAF19-06.

---

\* Electronic address: [Corresponding author: jqliao@hunnu.edu.cn](mailto:jqliao@hunnu.edu.cn)

- [1] T. J. Kippenberg and K. J. Vahala, Cavity optomechanics: Backaction at the mesoscale, *Science* **321**, 1172 (2008).
- [2] M. Aspelmeyer, T. J. Kippenberg, and F. Marquardt, Cavity optomechanics, *Rev. Mod. Phys.* **86**, 1391 (2014).
- [3] M. Metcalfe, Applications of cavity optomechanics, *Appl. Phys. Rev.* **1**, 031105 (2014).
- [4] S. Mancini, V. Giovannetti, D. Vitali, and P. Tombesi, Entangling Macroscopic Oscillators Exploiting Radiation Pressure, *Phys. Rev. Lett.* **88**, 120401 (2002).
- [5] K. Børkje, A. Nunnenkamp, and S. M. Girvin, Proposal for Entangling Remote Micromechanical Oscillators via Optical Measurements, *Phys. Rev. Lett.* **107**, 123601 (2011).
- [6] K. Stannigel, P. Komar, S. J. M. Habraken, S. D. Bennett, M. D. Lukin, P. Zoller, and P. Rabl, Optomechanical Quantum Information Processing with Photons and Phonons, *Phys. Rev. Lett.* **109**, 013603 (2012).
- [7] F. Massel, S. U. Cho, J.-M. Pirkkalainen, P. J. Hakonen, T. T. Heikkilä, and M. A. Sillanpää, Multimode circuit optomechanics near the quantum limit, *Nat. Commun.* **3**, 987 (2012).
- [8] N. Spethmann, J. Kohler, S. Schreppler, L. Buchmann, and D. M. Stamper-Kurn, Cavity-mediated coupling of mechanical oscillators limited by quantum backaction, *Nat. Phys.* **12**, 27 (2016).
- [9] P. Piergentili, L. Catalini, M. Bawaj, S. Zippilli, N. Malossi, R. Natali, D. Vitali, and G. Di Giuseppe, Two-membrane cavity optomechanics, *New J. Phys.* **20**, 083024 (2018).
- [10] R. Riedinger, A. Wallucks, I. Marinković, C. Löschnauer, M. Aspelmeyer, S. Hong, and S. Gröblacher, Remote quantum entanglement between two micromechanical oscillators, *Nature (London)* **556**, 473 (2018).
- [11] C. F. Ockeloen-Korppi, E. Damskägg, J.-M. Pirkkalainen, M. Asjad, A. A. Clerk, F. Massel, M. J. Woolley, and M. A. Sillanpää, Stabilized entanglement of massive mechanical oscillators, *Nature (London)* **556**, 478 (2018).
- [12] C. Yang, X. Wei, J. Sheng, and H. Wu, Phonon heat transport in cavity-mediated optomechanical nanoresonators, *Nat. Commun.* **11**, 4656 (2020).
- [13] S. Kotler, G. A. Peterson, E. Shojaei, F. Lecocq, K. Cicak, A. Kwiatkowski, S. Geller, S. Glancy, E. Knill, R. W. Simmonds, J. Aumentado, and J. D. Teufel, Direct observation of deterministic macroscopic entanglement, *Science* **372**, 622 (2021).
- [14] L. M. de Lépinay, C. F. Ockeloen-Korppi, M. J. Woolley, and M. A. Sillanpää, Quantum mechanics-free subsystem with mechanical oscillators, *Science* **372**, 625 (2021).
- [15] M. Bhattacharya and P. Meystre, Multiple membrane cavity optomechanics, *Phys. Rev. A* **78**, 041801(R) (2008).
- [16] A. Xuereb, C. Genes, and A. Dantan, Strong Coupling and Long-Range Collective Interactions in Optomechanical Arrays, *Phys. Rev. Lett.* **109**, 223601 (2012).
- [17] X.-W. Xu, Y.-J. Zhao, and Y.-X. Liu, Entangled-state engineering of vibrational modes in a multimembrane optomechanical system, *Phys. Rev. A* **88**, 022325 (2013).
- [18] A. Mari, A. Farace, N. Didier, V. Giovannetti, and R. Fazio, Measures of Quantum Synchronization in Continuous Variable Systems, *Phys. Rev. Lett.* **111**, 103605 (2013).
- [19] M. Zhang, S. Shah, J. Cardenas, and M. Lipson, Synchronization and Phase Noise Reduction in Micromechanical Oscillator Arrays Coupled through Light, *Phys. Rev. Lett.* **115**, 163902 (2015).
- [20] W. H. P. Nielsen, Y. Tsaturyan, C. B. Møller, E. S. Polzik, and A. Schliesser, Multimode optomechanical system in the quantum regime, *Proc. Natl. Acad. Sci. U.S.A.* **114**, 62 (2017).
- [21] L. Mercadé, K. Pelka, R. Burgwal, A. Xuereb, A. Martínez, and E. Verhagen, Floquet Phonon Lasing in Multimode Optomechanical Systems, *Phys. Rev. Lett.* **127**, 073601 (2021).
- [22] G. Heinrich, M. Ludwig, J. Qian, B. Kubala, and F. Marquardt, Collective Dynamics in Optomechanical Arrays, *Phys. Rev. Lett.* **107**, 043603 (2011).
- [23] M. Ludwig and F. Marquardt, Quantum Many-Body Dynamics in Optomechanical Arrays, *Phys. Rev. Lett.* **111**, 073603 (2013).
- [24] A. Xuereb, C. Genes, G. Pupillo, M. Paternostro, and A. Dantan, Reconfigurable Long-Range Phonon Dynamics in Optomechanical Arrays, *Phys. Rev. Lett.* **112**, 133604 (2014).
- [25] O. Černotík, S. Mahmoodian, and K. Hammerer, Spatially Adiabatic Frequency Conversion in Optoelectromechanical Arrays, *Phys. Rev. Lett.* **121**, 110506 (2018).
- [26] K. C. Schwab and M. L. Roukes, Putting mechanics into quantum mechanics, *Phys. Today* **58**(7), 36 (2005).
- [27] F. Massel, T. T. Heikkilä, J.-M. Pirkkalainen, S. U. Cho, H. Saloniemi, P. J. Hakonen, and M. A. Sillanpää, Microwave amplification with nanomechanical resonators, *Nature (London)* **480**, 351 (2011).
- [28] P. Huang, P. Wang, J. Zhou, Z. Wang, C. Ju, Z. Wang, Y. Shen, C. Duan, and J. Du, Demonstration of Motion Transduction Based on Parametrically Coupled Mechanical Resonators, *Phys. Rev. Lett.* **110**, 227202 (2013).
- [29] V. Peano, H. G. L. Schwefel, C. Marquardt, and F. Marquardt, Intracavity Squeezing Can Enhance Quantum-Limited Optomechanical Position Detection through Deamplification, *Phys. Rev. Lett.* **115**, 243603 (2015).
- [30] X.-W. Xu, Y.-x. Liu, C.-P. Sun, and Y. Li, Mechanical PT symmetry in coupled optomechanical systems, *Phys. Rev. A* **92**, 013852 (2015).
- [31] H. Xu, D. Mason, L. Jiang, and J. G. E. Harris, Topological energy transfer in an optomechanical system with exceptional points, *Nature (London)* **537**, 80 (2016).
- [32] Z. Shen, Y.-L. Zhang, Y. Chen, C.-L. Zou, Y.-F. Xiao, X.-B. Zou, F.-W. Sun, G.-C. Guo, and C.-H. Dong, Experimental realization of optomechanically induced non-reciprocity, *Nat. Photonics* **10**, 657 (2016).
- [33] K. Fang, J. Luo, A. Metelmann, M. H. Matheny, F. Marquardt, A. A. Clerk, and O. Painter, Generalized non-reciprocity in an optomechanical circuit via synthetic magnetism and reservoir engineering, *Nat. Phys.* **13**, 465 (2017).
- [34] D. Malz, L. D. Tóth, N. R. Bernier, A. K. Feofanov, T. J. Kippenberg, and A. Nunnenkamp, Quantum-Limited Directional Amplifiers with Optomechanics, *Phys. Rev. Lett.* **120**, 023601 (2018).
- [35] Z. Shen, Y.-L. Zhang, Y. Chen, F.-W. Sun, X.-B. Zou, G.-C. Guo, C.-L. Zou, and C.-H. Dong, Reconfigurable optomechanical circulator and directional amplifier, *Nat. Commun.* **9**, 1797 (2018).
- [36] J. P. Mathew, J. d. Pino, and E. Verhagen, Synthetic gauge fields for phonon transport in a nano-optomechanical system, *Nat.*

- Nanotechnol. **15**, 198 (2020).
- [37] H. Xu, L. Jiang, A. A. Clerk, and J. G. E. Harris, Nonreciprocal control and cooling of phonon modes in an optomechanical system, *Nature (London)* **568**, 65 (2019).
  - [38] I. Wilson-Rae, N. Nooshi, W. Zwerger, and T. J. Kippenberg, Theory of Ground State Cooling of a Mechanical Oscillator Using Dynamical Backaction, *Phys. Rev. Lett.* **99**, 093901 (2007).
  - [39] F. Marquardt, J. P. Chen, A. A. Clerk, and S. M. Girvin, Quantum Theory of Cavity-Assisted Sideband Cooling of Mechanical Motion, *Phys. Rev. Lett.* **99**, 093902 (2007).
  - [40] C. Genes, D. Vitali, P. Tombesi, S. Gigan, and M. Aspelmeyer, Ground-state cooling of a micromechanical oscillator: Comparing cold damping and cavity-assisted cooling schemes, *Phys. Rev. A* **77**, 033804 (2008); **79**, 039903(E) (2009).
  - [41] J. Chan, T. P. M. Alegre, A. H. Safavi-Naeini, J. T. Hill, A. Krause, S. Gröblacher, M. Aspelmeyer, and O. Painter, Laser cooling of a nanomechanical oscillator into its quantum ground state, *Nature (London)* **478**, 89 (2011).
  - [42] J. D. Teufel, T. Donner, D. Li, J. W. Harlow, M. S. Allman, K. Cicak, A. J. Sirois, J. D. Whittaker, K. W. Lehnert, and R. W. Simmonds, Sideband cooling of micromechanical motion to the quantum ground state, *Nature (London)* **475**, 359 (2011).
  - [43] Y.-C. Liu, Y.-F. Xiao, X. Luan, and C. W. Wong, Dynamic Dissipative Cooling of a Mechanical Resonator in Strong Coupling Optomechanics, *Phys. Rev. Lett.* **110**, 153606 (2013).
  - [44] X. Xu, T. Purdy, and J. M. Taylor, Cooling a Harmonic Oscillator by Optomechanical Modification of Its Bath, *Phys. Rev. Lett.* **118**, 223602 (2017).
  - [45] J. B. Clark, F. Lecocq, R. W. Simmonds, J. Aumentado, and J. D. Teufel, Sideband cooling beyond the quantum backaction limit with squeezed light, *Nature (London)* **541**, 191 (2017).
  - [46] L. Qiu, I. Shomroni, P. Seidler, and T. J. Kippenberg, Laser Cooling of a Nanomechanical Oscillator to Its Zero-Point Energy, *Phys. Rev. Lett.* **124**, 173601 (2020).
  - [47] M. Rossi, D. Mason, J. Chen, Y. Tsaturyan, and A. Schliesser, Measurement-based quantum control of mechanical motion, *Nature (London)* **563**, 53 (2018).
  - [48] F. Tebbenjohanns, M. Frimmer, A. Militaru, V. Jain, and L. Novotny, Cold Damping of an Optically Levitated Nanoparticle to Microkelvin Temperatures, *Phys. Rev. Lett.* **122**, 223601 (2019).
  - [49] J. Guo, R. Norte, and S. Gröblacher, Feedback Cooling of a Room Temperature Mechanical Oscillator close to its Motional Ground State, *Phys. Rev. Lett.* **123**, 223602 (2019).
  - [50] C. Genes, D. Vitali, and P. Tombesi, Simultaneous cooling and entanglement of mechanical modes of amicromirror in an optical cavity, *New J. Phys.* **10**, 095009 (2008).
  - [51] A. B. Shkarin, N. E. Flowers-Jacobs, S. W. Hoch, A. D. Kashkanova, C. Deutsch, J. Reichel, and J. G. E. Harris, Optically Mediated Hybridization between Two Mechanical Modes, *Phys. Rev. Lett.* **112**, 013602 (2014).
  - [52] M. C. Kuzyk and H. Wang, Controlling multimode optomechanical interactions via interference, *Phys. Rev. A* **96**, 023860 (2017).
  - [53] C. F. Ockeloen-Korppi, M. F. Gely, E. Damskägg, M. Jenkins, G. A. Steele, and M. A. Sillanpää, Sideband cooling of nearly degenerate micromechanical oscillators in a multimode optomechanical system, *Phys. Rev. A* **99**, 023826 (2019).
  - [54] C. Dong, V. Fiore, M. C. Kuzyk, and H. Wang, Optomechanical dark mode, *Science* **338**, 1609 (2012).
  - [55] Y.-D. Wang and A. A. Clerk, Using Interference for High Fidelity Quantum State Transfer in Optomechanics, *Phys. Rev. Lett.* **108**, 153603 (2012).
  - [56] L. Tian, Adiabatic State Conversion and Pulse Transmission in Optomechanical Systems, *Phys. Rev. Lett.* **108**, 153604 (2012).
  - [57] D. P. Lake, M. Mitchell, B. C. Sanders, and P. E. Barclay, Two-colour interferometry and switching through optomechanical dark mode excitation, *Nat. Commun.* **11**, 1 (2020).
  - [58] D.-G. Lai, F. Zou, B.-P. Hou, Y.-F. Xiao, and J.-Q. Liao, Simultaneous cooling of coupled mechanical resonators in cavity optomechanics, *Phys. Rev. A* **98**, 023860 (2018).
  - [59] D.-G. Lai, J. Huang, B.-P. Hou, F. Nori, and J.-Q. Liao, Domino cooling of a coupled mechanical-resonator chain via cold-damping feedback, *Phys. Rev. A* **103**, 063509 (2021).
  - [60] C. Sommer and C. Genes, Partial Optomechanical Refrigeration via Multimode Cold-Damping Feedback, *Phys. Rev. Lett.* **123**, 203605 (2019).
  - [61] C. Sommer, A. Ghosh, and C. Genes, Multimode cold-damping optomechanics with delayed feedback, *Phys. Rev. Research* **2**, 033299 (2020).
  - [62] D.-G. Lai, J.-F. Huang, X.-L. Yin, B.-P. Hou, W. Li, D. Vitali, F. Nori, and J.-Q. Liao, Nonreciprocal ground-state cooling of multiple mechanical resonators, *Phys. Rev. A* **102**, 011502(R) (2020).
  - [63] M. T. Naseem and Ö. E. Müstecaplıoğlu, Ground-state cooling of mechanical resonators by quantum reservoir engineering, *Commun. Phys.* **4**, 95 (2021).
  - [64] M. O. Scully and M. S. Zubairy, *Quantum Optics* (Cambridge University Press, Cambridge, 1997).
  - [65] See Supplemental Material for details about the simultaneous ground-state cooling of two mechanical modes in both an “ $N$ ”-type and a network-coupled four-mode optomechanical system, the general dark-mode breaking conditions, and the simultaneous ground-state cooling of  $N$  mechanical modes in a multiple-mechanical-mode optomechanical system. Concretely, we present the detailed derivation of the Langevin equations, the analysis of the stability condition, the calculation of the covariance matrix, and the derivation of the parameter condition for forming and breaking the dark modes.
  - [66] I. S. Gradshteyn and I. M. Ryzhik, *Table of Integrals, Series, and Products* (Academic, New York, 2014).
  - [67] C. W. Gardiner and P. Zoller, *Quantum Noise* (Springer, Berlin, 2000).
  - [68] G. S. Agarwal, *Quantum Optics* (Cambridge University Press, Cambridge, 2013).
  - [69] D. Vitali, S. Gigan, A. Ferreira, H. R. Böhm, P. Tombesi, A. Guerreiro, V. Vedral, A. Zeilinger, and M. Aspelmeyer, Optomechanical Entanglement Between a Movable Mirror and a Cavity Field, *Phys. Rev. Lett.* **98**, 030405 (2007).
  - [70] Q. Lin, J. Rosenberg, D. Chang, R. Camacho, M. Eichenfield, K. J. Vahala, and O. Painter, Coherent mixing of mechanical excitations in nano-optomechanical structures, *Nat. Photonics* **4**, 236 (2010).

# Supplementary Material for “Multimode Optomechanical Cooling via General Dark-Mode Control”

Jian Huang<sup>1</sup>, Deng-Gao Lai<sup>2</sup>, Cheng Liu<sup>1</sup>, Jin-Feng Huang<sup>1</sup>, Franco Nori<sup>2,3,4</sup>, and Jie-Qiao Liao<sup>1,\*</sup>

<sup>1</sup>Key Laboratory of Low-Dimensional Quantum Structures and Quantum Control of Ministry of Education,  
Key Laboratory for Matter Microstructure and Function of Hunan Province,  
Department of Physics and Synergetic Innovation Center for Quantum Effects and Applications,  
Hunan Normal University, Changsha 410081, China

<sup>2</sup>Theoretical Quantum Physics Laboratory, RIKEN Cluster for Pioneering Research, Wako-shi, Saitama 351-0198, Japan

<sup>3</sup>RIKEN Center for Quantum Computing (RQC), 2-1 Hirosawa, Wako-shi, Saitama 351-0198, Japan

<sup>4</sup>Physics Department, The University of Michigan, Ann Arbor, Michigan 48109-1040, USA

This supplementary material is composed of three sections. In section **S1**, we study the simultaneous ground-state cooling of two mechanical modes in an “ $N$ ”-type coupled four-mode optomechanical system. Concretely, we derive the quantum Langevin equations, analyze the stability conditions, and study the cooling performance of the two mechanical modes in this system. In section **S2**, we study the ground-state cooling and the general dark-mode-breaking conditions in a network-coupled four-mode optomechanical system consisting of two cavity modes and two mechanical modes. By considering fourteen coupling configurations, we clarify the necessary couplings for realizing the ground-state cooling of the two mechanical modes. We also derive the analytical parameter conditions for forming the dark mode. In section **S3**, we consider the simultaneous ground-state cooling of multiple mechanical modes and the dark-mode breaking in a multiple-mechanical-mode optomechanical system.

## S1. SIMULTANEOUS GROUND-STATE COOLING OF TWO MECHANICAL MODES IN THE “ $N$ ”-TYPE COUPLED FOUR-MODE OPTOMECHANICAL SYSTEM

### A. Equations of motion and semiclassical motion

The Hamiltonian of the “ $N$ ”-type coupled four-mode optomechanical system (see Fig. **S1**) considered in the main text reads ( $\hbar = 1$ )

$$H(t) = \omega_c a^\dagger a + \omega_s a_s^\dagger a_s + \sum_{l=1,2} [\omega_l b_l^\dagger b_l + g_l a^\dagger a (b_l^\dagger + b_l)] + g_{s1} a_s^\dagger a_s (b_1^\dagger + b_1) + (\Omega a^\dagger e^{-i\omega_L t} + \Omega_s a_s^\dagger e^{-i\omega_d t} + \text{H.c.}), \quad (\text{S1})$$

where  $a$  ( $a^\dagger$ ),  $a_s$  ( $a_s^\dagger$ ), and  $b_{l=1,2}$  ( $b_l^\dagger$ ) are, respectively, the annihilation (creation) operators of the intermediate cavity field, the auxiliary cavity field, and the  $l$ th mechanical mode, with the corresponding resonance frequencies  $\omega_c$ ,  $\omega_s$ , and  $\omega_l$ . The  $g_{l=1,2}$  ( $g_{s1}$ ) term in Eq. (S1) describes the optomechanical coupling between the mechanical mode  $b_{l=1,2}$  ( $b_1$ ) and the cavity field  $a$  ( $a_s$ ). Besides, the cavity-field mode  $a$  ( $a_s$ ) is strongly driven by the laser field with the driving frequency  $\omega_L$  ( $\omega_d$ ) and the driving amplitude  $\Omega$  ( $\Omega_s$ ). In a rotating frame defined by the transformation operator  $\exp[-i(\omega_L a^\dagger a + \omega_d a_s^\dagger a_s)t]$ , the Hamiltonian in Eq. (S1) becomes

$$H_I = \Delta_c a^\dagger a + \Delta_s a_s^\dagger a_s + \sum_{l=1,2} [\omega_l b_l^\dagger b_l + g_l a^\dagger a (b_l^\dagger + b_l)] + g_{s1} a_s^\dagger a_s (b_1^\dagger + b_1) + (\Omega a^\dagger + \Omega_s a_s^\dagger + \text{H.c.}), \quad (\text{S2})$$

where  $\Delta_c = \omega_c - \omega_L$  ( $\Delta_s = \omega_s - \omega_d$ ) is the driving detuning of the cavity-mode frequency  $\omega_c$  ( $\omega_s$ ) with respect to its driving frequency  $\omega_L$  ( $\omega_d$ ).

Assume that the two cavity-field modes are coupled to individual vacuum baths, and that the two mechanical modes are coupled to individual heat baths, then the evolution of this system is governed by the quantum Langevin equations

$$\dot{a} = -(i\Delta_c + \kappa)a - i\Omega - i \sum_{l=1,2} g_l a (b_l^\dagger + b_l) + \sqrt{2\kappa} a_{\text{in}}, \quad (\text{S3a})$$

$$\dot{a}_s = -(i\Delta_s + \kappa_s)a_s - i[\Omega_s + g_{s1}a_s(b_1^\dagger + b_1)] + \sqrt{2\kappa_s} a_{s,\text{in}}, \quad (\text{S3b})$$

$$\dot{b}_1 = -(\gamma_1 + i\omega_1)b_1 - i(g_1 a^\dagger a + g_{s1} a_s^\dagger a_s) + \sqrt{2\gamma_1} b_{1,\text{in}}, \quad (\text{S3c})$$

$$\dot{b}_2 = -(\gamma_2 + i\omega_2)b_2 - ig_2 a^\dagger a + \sqrt{2\gamma_2} b_{2,\text{in}}, \quad (\text{S3d})$$

where  $\kappa$ ,  $\kappa_s$ , and  $\gamma_{l=1,2}$  are the decay rates of the intermediate cavity mode  $a$ , the auxiliary cavity mode  $a_s$ , and the  $l$ th mechanical mode  $b_{l=1,2}$ , respectively. The operators  $a_{\text{in}}$  ( $a_{\text{in}}^\dagger$ ),  $a_{s,\text{in}}$  ( $a_{s,\text{in}}^\dagger$ ), and  $b_{l,\text{in}}$  ( $b_{l,\text{in}}^\dagger$ ) are the noise operators associated with the



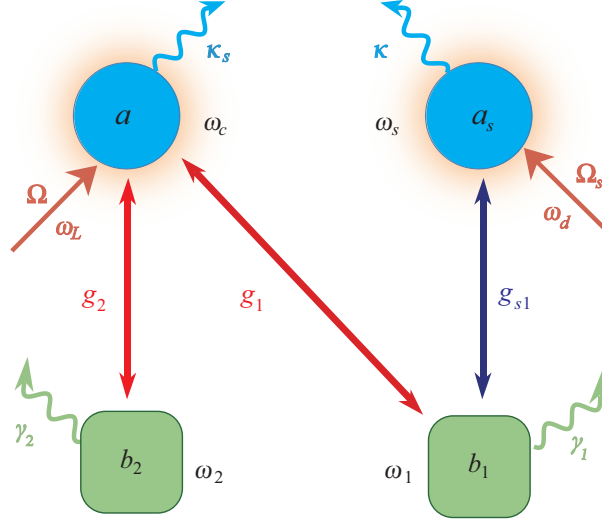


FIG. S1: Schematic of the “N”-type coupled four-mode optomechanical system. An intermediate coupling cavity mode  $a$  with resonance frequency  $\omega_c$  is optomechanically coupled to two mechanical modes  $b_1$  and  $b_2$  with the corresponding resonance frequencies  $\omega_1$  and  $\omega_2$ . An auxiliary cavity mode  $a_s$  with the resonance frequency  $\omega_s$  is optomechanically coupled to the mechanical mode  $b_1$ . The coupling strength between the cavity mode  $a$  ( $a_s$ ) and the mechanical mode  $b_{l=1,2}$  ( $b_1$ ) is denoted by  $g_{l=1,2}$  ( $g_{s1}$ ). The cavity mode  $a$  ( $a_s$ ) is driven by a monochromatic field with the driving frequency  $\omega_L$  ( $\omega_d$ ) and the driving amplitude  $\Omega$  ( $\Omega_s$ ). The decay rates of the intermediate cavity mode, the auxiliary cavity mode, and the two mechanical modes are denoted by  $\kappa$ ,  $\kappa_s$ , and  $\gamma_{l=1,2}$ , respectively.

intermediate cavity mode, the auxiliary cavity mode, and the  $l$ th mechanical mode, respectively. These noise operators have zero mean values and obey the following correlation functions,

$$\langle a_{\text{in}}(t)a_{\text{in}}^\dagger(t') \rangle = \delta(t-t'), \quad \langle a_{\text{in}}^\dagger(t)a_{\text{in}}(t') \rangle = 0, \quad (\text{S4a})$$

$$\langle a_{s,\text{in}}(t)a_{s,\text{in}}^\dagger(t') \rangle = \delta(t-t'), \quad \langle a_{s,\text{in}}^\dagger(t)a_{s,\text{in}}(t') \rangle = 0, \quad (\text{S4b})$$

$$\langle b_{l,\text{in}}(t)b_{l,\text{in}}^\dagger(t') \rangle = (\bar{n}_l + 1)\delta(t-t'), \quad \langle b_{l,\text{in}}^\dagger(t)b_{l,\text{in}}(t') \rangle = \bar{n}_l\delta(t-t'), \quad (\text{S4c})$$

for  $l = 1, 2$ , where  $\bar{n}_{l=1,2}$  is the average thermal-phonon occupation number associated with the  $l$ th mechanical mode.

To cool the mechanical modes, we assume that the two cavity modes are driven strongly, then the mean photon numbers in the two cavities are large enough and this four-mode optomechanical system can be processed by the linearization procedure. In this way, the operators  $o \in \{a, a^\dagger, a_s, a_s^\dagger, b_l, b_l^\dagger\}$  can be expressed as a sum of steady-state average values and quantum fluctuations, i.e.,  $o = \langle o \rangle_{\text{ss}} + \delta o$ . By separating the steady-state average values and the quantum fluctuations, we can obtain the linearized Langevin equations of the quantum fluctuations as

$$\delta \dot{a} = -(\kappa + i\Delta'_c)\delta a - i \sum_{l=1,2} [G_l(\delta b_l + \delta b_l^\dagger)] + \sqrt{2\kappa}a_{\text{in}}, \quad (\text{S5a})$$

$$\delta \dot{a}_s = -(\kappa_s + i\Delta'_s)\delta a_s - iG_{s1}(\delta b_1 + \delta b_1^\dagger) + \sqrt{2\kappa_s}a_{s,\text{in}}, \quad (\text{S5b})$$

$$\delta \dot{b}_1 = -(i\omega_1 + \gamma_1)\delta b_1 - iG_1^*\delta a - iG_1\delta a^\dagger - iG_{s1}^*\delta a_s - iG_{s1}\delta a_s^\dagger + \sqrt{2\gamma_1}b_{1,\text{in}}, \quad (\text{S5c})$$

$$\delta \dot{b}_2 = -(i\omega_2 + \gamma_2)\delta b_2 - iG_2^*\delta a - iG_2\delta a^\dagger + \sqrt{2\gamma_2}b_{2,\text{in}}, \quad (\text{S5d})$$

where  $\delta a$  ( $\delta a^\dagger$ ),  $\delta a_s$  ( $\delta a_s^\dagger$ ), and  $\delta b_{l=1,2}$  ( $\delta b_l^\dagger$ ) are the annihilation (creation) fluctuation operators of the intermediate cavity mode, the auxiliary cavity mode, and the  $l$ th mechanical mode, respectively. In addition, we introduce the effective driving detunings of the cavity mode  $a$  and the auxiliary cavity mode  $a_s$  as

$$\Delta'_c = \Delta_c + 2g_1\text{Re}[\beta_1] + 2g_2\text{Re}[\beta_2], \quad (\text{S6a})$$

$$\Delta'_s = \Delta_s + 2g_{s1}\text{Re}[\beta_1], \quad (\text{S6b})$$

where  $\text{Re}[\beta_{l=1,2}]$  takes the real part of  $\beta_l$ , and  $G_l = g_l\alpha$  ( $G_{s1} = g_{s1}\alpha_s$ ) is the linearized optomechanical-coupling strength between the cavity mode  $a$  ( $a_s$ ) and the  $l$ th mechanical mode (the mechanical mode  $b_1$ ). In the steady-state case, the average values of the



system operators can be obtained as

$$\alpha \equiv \langle a \rangle_{ss} = \frac{-i\Omega}{\kappa + i\Delta'_c}, \quad (S7a)$$

$$\alpha_s \equiv \langle a_s \rangle_{ss} = \frac{-i\Omega_s}{\kappa_s + i\Delta'_s}, \quad (S7b)$$

$$\beta_1 \equiv \langle b_1 \rangle_{ss} = \frac{-ig_1|\alpha|^2 - ig_{s1}|\alpha_s|^2}{\gamma_1 + i\omega_1}, \quad (S7c)$$

$$\beta_2 \equiv \langle b_2 \rangle_{ss} = \frac{-ig_2|\alpha|^2}{\gamma_2 + i\omega_2}. \quad (S7d)$$

For convenience, we will assume that the steady-state values of  $\alpha$  and  $\alpha_s$  are real by choosing proper phases of the driving amplitudes  $\Omega$  and  $\Omega_s$ , so the linearized optomechanical-coupling strengths  $G_{l=1,2}$  and  $G_{s1}$  are also real. We denote  $\Omega = |\Omega|e^{i\theta}$  and  $\Omega_s = |\Omega_s|e^{i\theta_s}$ , where  $\theta$  and  $\theta_s$  are chosen such that  $\alpha$  and  $\alpha_s$  are real. Then the real variables are obtained as

$$\alpha = \frac{-|\Omega|}{\sqrt{\kappa^2 + \Delta_c'^2}}, \quad (S8a)$$

$$\alpha_s = \frac{-|\Omega_s|}{\sqrt{\kappa_s^2 + \Delta_s'^2}}, \quad (S8b)$$

$$\text{Re}[\beta_1] = \frac{-\omega_1(g_1|\alpha|^2 + g_{s1}|\alpha_s|^2)}{\gamma_1^2 + \omega_1^2}, \quad (S8c)$$

$$\text{Re}[\beta_2] = \frac{-\omega_2 g_2 |\alpha|^2}{\gamma_2^2 + \omega_2^2}. \quad (S8d)$$

Here, we can see from Eq. (S8) that the coupling strengths depend on the driving amplitudes when the driving detunings  $\Delta'_c$  and  $\Delta'_s$  take certain values. Then the linearized optomechanical-coupling strengths can be tuned by controlling the driving amplitudes.

## B. Stability analysis

For studying quantum cooling of the mechanical modes, we are interested in the steady-state properties of the system. Therefore, we should analyze the stability condition of this linearized system. To this end, we rewrite the linearized Langevin equations (S5) as the following compact form

$$\dot{\mathbf{u}}(t) = \mathbf{A}\mathbf{u}(t) + \mathbf{N}(t), \quad (S9)$$

where  $\mathbf{u}(t)$ ,  $\mathbf{A}$ , and  $\mathbf{N}(t)$  are, respectively, the fluctuation operator vector, coefficient matrix, and noise operator vector, which take the form as

$$\mathbf{u}(t) = [\delta a(t), \delta a_s(t), \delta b_1(t), \delta b_2(t), \delta a^\dagger(t), \delta a_s^\dagger(t), \delta b_1^\dagger(t), \delta b_2^\dagger(t)]^T, \quad (S10)$$

$$\mathbf{N}(t) = \sqrt{2}[\sqrt{\kappa}a_{\text{in}}(t), \sqrt{\kappa_s}a_{s,\text{in}}(t), \sqrt{\gamma_1}b_{1,\text{in}}(t), \sqrt{\gamma_2}b_{2,\text{in}}(t), \sqrt{\kappa}a_{\text{in}}^\dagger(t), \sqrt{\kappa_s}a_{s,\text{in}}^\dagger(t), \sqrt{\gamma_1}b_{1,\text{in}}^\dagger(t), \sqrt{\gamma_2}b_{2,\text{in}}^\dagger(t)]^T, \quad (S11)$$

and

$$\mathbf{A} = \begin{pmatrix} -(\kappa + i\Delta'_c) & 0 & -iG_1 & -iG_2 & 0 & 0 & -iG_1 & -iG_2 \\ 0 & -(i\Delta'_s + \kappa_s) & -iG_{s1} & 0 & 0 & 0 & -iG_{s1} & 0 \\ -iG_1^* & -iG_{s1}^* & -(i\omega_1 + \gamma_1) & 0 & -iG_1 & -iG_{s1} & 0 & 0 \\ -iG_2^* & 0 & 0 & -(i\omega_2 + \gamma_2) & -iG_2 & 0 & 0 & 0 \\ 0 & 0 & iG_1^* & iG_2^* & -(\kappa - i\Delta'_c) & 0 & iG_1^* & iG_2^* \\ 0 & 0 & iG_{s1}^* & 0 & 0 & -(\kappa_s - i\Delta'_s) & iG_{s1}^* & 0 \\ iG_1^* & iG_{s1}^* & 0 & 0 & iG_1 & iG_{s1} & -(\gamma_1 - i\omega_1) & 0 \\ iG_2^* & 0 & 0 & 0 & iG_2 & 0 & 0 & -(\gamma_2 - i\omega_2) \end{pmatrix}. \quad (S12)$$

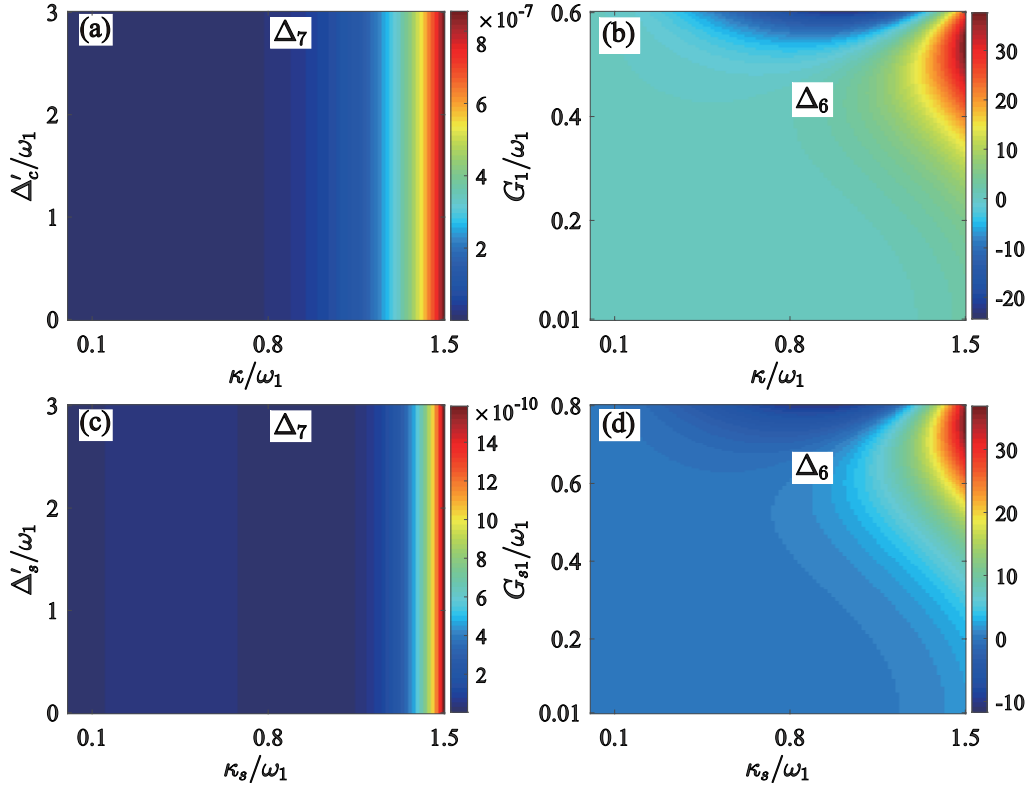


FIG. S2: Stability conditions of parameters. The value of the determinant (a) [(c)]  $\Delta_7$  of the coefficients ( $b_1$ - $b_8$ ) versus the scaled driving detuning  $\Delta'_c/\omega_1$  ( $\Delta'_s/\omega_1$ ) and the scaled cavity-field decay rate  $\kappa/\omega_1$  ( $\kappa_s/\omega_1$ ). The value of the determinant (b) [(d)]  $\Delta_6$  versus the scaled linearized optomechanical coupling strength  $G_1/\omega_1$  ( $G_{s1}/\omega_1$ ) and the scaled decay rate  $\kappa/\omega_1$  ( $\kappa_s/\omega_1$ ). Note that the value of the determinant  $\Delta_6$  ( $\Delta_7$ ) is smallest among the determinants  $\Delta_1$ - $\Delta_8$  when we choose two certain parameters as variables (such as  $\kappa/\omega_1$  and  $\Delta'_c/\omega_1$ ). When the parameters are not used as variables, the values are  $\omega_2/\omega_1 = 1$ ,  $\Delta'_s/\omega_1 = \Delta'_c/\omega_1 = 1$ ,  $\kappa_s/\omega_1 = \kappa/\omega_1 = 0.1$ ,  $\gamma_1/\omega_1 = \gamma_2/\omega_1 = 10^{-5}$ ,  $G_1/\omega_1 = G_2/\omega_1 = 0.05$ , and  $G_{s1}/\omega_1 = 0.08$ .

In Eqs. (S10) and (S11), the superscript “ $T$ ” denotes the matrix transpose. The eigensystem of the coefficient matrix  $\mathbf{A}$  determines the stability of the system. By using the Routh-Hurwitz criterion, we can find the stability condition. The stability of the system is determined by the eigensystem of the coefficient matrix  $\mathbf{A}$  given by Eq. (S12). Based on the eigenequation

$$\mathbf{A}\mathbf{x} = \lambda\mathbf{x}, \quad (\text{S13})$$

the eigenvalues can be obtained by solving the equation

$$|\mathbf{A} - \lambda\mathbf{I}| = 0, \quad (\text{S14})$$

which leads to the equation

$$F(\lambda) = \sum_{n=0}^8 b_{8-n}\lambda^n = 0. \quad (\text{S15})$$

Here, we introduce the coefficients

$$\begin{aligned}
b_0 &= 1, \\
b_1 &= 2(\kappa + \kappa_s + 2\gamma_1), \\
b_2 &= (\kappa + \kappa_s + 8\gamma_1)(\kappa + \kappa_s) + 2\kappa\kappa_s + 6\gamma_1^2 + 2\omega_1^2 + \Delta_c'^2 + \Delta_s'^2, \\
b_3 &= 4\kappa_s^2\gamma_1 + 2\kappa^2(\kappa_s + 2\gamma_1) + 2\kappa_s(6\gamma_1^2 + 2\omega_1^2 + \Delta_c'^2) + 2\kappa(\kappa_s^2 + 8\kappa_s\gamma_1 + 6\gamma_1^2 + 2\omega_1^2 + \Delta_s'^2) + 4\gamma_1(\gamma_1^2 + \omega_1^2 + \Delta_c'^2 + \Delta_s'^2), \\
b_4 &= (\gamma_1^2 + \omega_1^2)^2 - 4\omega_1(2G_1^2\Delta_c' - G_s^2\Delta_s') + 6\gamma_1^2\Delta_c'^2 + 2\omega_1^2\Delta_c'^2 + 8\kappa_s\gamma_1(\gamma_1^2 + \omega_1^2 + \Delta_c'^2) + (\kappa_s^2 + \Delta_s'^2)(6\gamma_1^2 + 2\omega_1^2 + \Delta_c'^2) \\
&\quad + \kappa^2(\kappa_s^2 + 8\kappa_s\gamma_1 + 6\gamma_1^2 + 2\omega_1^2 + \Delta_s'^2) + 8\kappa[\kappa_s^2\gamma_1 + \kappa_s(3\gamma_1^2 + \omega_1^2) + \gamma_1(\gamma_1^2 + \omega_1^2 + \Delta_s'^2)], \\
b_5 &= 4\kappa^2[\kappa_s^2\gamma_1 + \kappa_s(3\gamma_1^2 + \omega_1^2) + \gamma_1(\gamma_1^2 + \omega_1^2 + \Delta_s'^2)] + 2\kappa_s[(r_1^2 + \omega_1^2)^2 - 8G_1^2\omega_1\Delta_c' + 2(3\gamma_1^2 + \omega_1^2)\Delta_c'^2] \\
&\quad + 4\kappa_s^2\gamma_1(\gamma_1^2 + \omega_1^2 + \Delta_c'^2) + 2\kappa[8\kappa_s\gamma_1(\gamma_1^2 + \omega_1^2) + (r_1^2 + \omega_1^2)^2 + (2\kappa_s^2 + 2\Delta_s'^2)(3r_1^2 + \omega_1^2) - 4G_s^2\omega_1\Delta_s'] \\
&\quad + 4\gamma_1\{\Delta_c'[-4G_1^2\omega_1 + (\gamma_1^2 + \omega_1^2)\Delta_c'] - 2G_s^2\omega_1\Delta_s' + (\gamma_1^2 + \omega_1^2 + \Delta_c'^2)\Delta_s'^2\}, \\
b_6 &= (\gamma_1^2 + \omega_1^2)^2(\Delta_c'^2 + \kappa_s^2) + 8(\gamma_1^2 + \omega_1^2)(\kappa_s\gamma_1\Delta_c' - G_1^2\omega_1\Delta_c') - 8\kappa_sG_1^2\omega_1\Delta_c'(4\gamma_1 - \kappa_s) + 2\kappa_s^2(3\gamma_1^2 + \omega_1^2)\Delta_c'^2 \\
&\quad + [(\gamma_1^2 + \omega_1^2)^2 - 8G_1^2\omega_1\Delta_c' + 2(3\gamma_1^2 + \omega_1^2)\Delta_c'^2]\Delta_s'^2 + 4\kappa[(\gamma_1^2 + \omega_1^2)(2\kappa_s^2\gamma_1 + \kappa_s\gamma_1^2 + \kappa_s\omega_1^2 + 2\gamma_1\Delta_s'^2) - 4G_s^2\gamma_1\omega_1\Delta_s'] \\
&\quad + \kappa^2[(8\kappa_s\gamma_1 + \gamma_1^2 + \omega_1^2)(\gamma_1^2 + \omega_1^2) + (2\kappa_s^2 + 2\Delta_s'^2)(3\gamma_1^2 + \omega_1^2) - 4G_s^2\omega_1\Delta_s'] - 4G_s^2\omega_1(\gamma_1^2 + \omega_1^2 + \Delta_c'^2)\Delta_s', \\
b_7 &= 2\kappa^2[(\gamma_1^2 + \omega_1^2)(2\kappa_s^2\gamma_1 + \kappa_s\gamma_1^2 + \kappa_s\omega_1^2 + 2\gamma_1\Delta_s'^2) - 4G_s^2\gamma_1\omega_1\Delta_s'] + 2\kappa(\gamma_1^2 + \omega_1^2)[(\gamma_1^2 + \omega_1^2)(\kappa_s^2 + \Delta_s'^2) - 4G_s^2\omega_1\Delta_s'] \\
&\quad + 2\Delta_c'\{-8G_1^2\omega_1[\kappa_s\gamma_1(\kappa_s + \gamma_1) + \kappa_s\omega_1^2 + \gamma_1\Delta_s'^2] + \Delta_c'[(\gamma_1^2 + \omega_1^2)(2\kappa_s^2\gamma_1 + \kappa_s\gamma_1^2 + \kappa_s\omega_1^2 + 2\gamma_1\Delta_s'^2) - 4G_s^2\gamma_1\omega_1\Delta_s']\}, \\
b_8 &= \kappa^2(\gamma_1^2 + \omega_1^2)[(\gamma_1^2 + \omega_1^2)(\kappa_s^2 + \Delta_s'^2) - 4G_s\gamma_1\omega_1\Delta_s'] + \Delta_c'(\gamma_1^2 + \omega_1^2)[(\gamma_1^2 + \omega_1^2)(\kappa_s^2 + \Delta_s'^2) - 4G_s^2\omega_1\Delta_s'] \\
&\quad - 8\Delta_c'G_1^2\omega_1[(\gamma_1^2 + \omega_1^2)(\kappa_s^2 + \Delta_s'^2) - 2G_s^2\omega_1\Delta_s'].
\end{aligned} \tag{S16}$$

For simplicity, below we select the parameter conditions:  $G_1 = G_2$ ,  $\omega_1 = \omega_2$ , and  $\gamma_1 = \gamma_2$ . According to the Routh-Hurwitz criteria, the conditions for making sure that all of the roots of the equation  $F(\lambda) = 0$  are negative or have negative real parts are

$$\Delta_n = \begin{vmatrix} b_1 & 1 & 0 & 0 & 0 & 0 & \dots & 0 \\ b_3 & b_2 & b_1 & 1 & 0 & 0 & \dots & 0 \\ b_5 & b_4 & b_3 & b_2 & b_1 & 1 & \dots & 0 \\ \dots & \dots & \dots & \dots & \dots & \dots & \dots & \dots \\ b_{2n-1} & b_{2n-2} & b_{2n-3} & b_{2n-4} & b_{2n-5} & b_{2n-6} & \dots & b_n \end{vmatrix} > 0, \tag{S17}$$

for  $n = 1-8$ .

To make sure that the parameters we used in the subsequent numerical calculations are in the steady-state range, in Fig. S2 we plot the values of the determinants as functions of several parameters  $\kappa/\omega_1$ ,  $\kappa_s/\omega_1$ ,  $\Delta_c'/\omega_1$ ,  $\Delta_s'/\omega_1$ ,  $G_1/\omega_1$ , and  $G_{s1}/\omega_1$ . Here we only show the smallest numerical result of the determinant among the determinants  $\Delta_1$ - $\Delta_8$ . In Figs. S2(a) and S2(c), we can see that the values of  $\Delta_7$  increase when increasing the scaled cavity-field decay rate  $\kappa/\omega_1$  and  $\kappa_s/\omega_1$ . This means that regardless if the mechanical resonator is in the resolved-sideband limit or not, the parameters  $\kappa/\omega_1$  and  $\kappa_s/\omega_1$  are in steady-state range ( $\Delta_7 > 0$ ). In Figs. S2(b) and S2(d), we can see that the values of  $\Delta_6$  become negative when increasing the scaled linearized optomechanical-coupling strengths. This means that when the linearized optomechanical-coupling strengths  $G_1/\omega_1 > 0.4$  or  $G_{s1}/\omega_1 > 0.6$ , the parameters  $G_1/\omega_1$  and  $G_{s1}/\omega_1$  are not in the steady-state range ( $\Delta_6 < 0$ ). Therefore, the amplitudes of the driving fields we choose cannot be too large in the following numerical simulations.

### C. Simultaneous ground-state cooling of the two mechanical modes

In this subsection, we study the cooling performance of the two mechanical modes by calculating the final mean phonon numbers. To this end, we need to solve the steady state of the system. The formal solution of the linearized Langevin equations (S9) can be obtained as

$$\mathbf{u}(t) = \mathbf{M}(t)\mathbf{u}(0) + \int_0^t \mathbf{M}(t-s)\mathbf{N}(s)ds, \tag{S18}$$

where we introduce the matrix  $\mathbf{M}(t) = \exp(\mathbf{A}t)$ . The final mean phonon numbers of the two mechanical modes can be calculated by solving the steady state of the system.

Based on Eq. (S18), we can obtain the final mean phonon numbers by solving the Lyapunov equation. To this end, we introduce the covariance matrix  $\mathbf{V}$  of the system by defining the matrix elements as

$$\mathbf{V}_{ij} = \frac{1}{2}[\langle \mathbf{u}_i(\infty)\mathbf{u}_j(\infty) \rangle + \langle \mathbf{u}_j(\infty)\mathbf{u}_i(\infty) \rangle], \quad i, j = 1-8. \tag{S19}$$

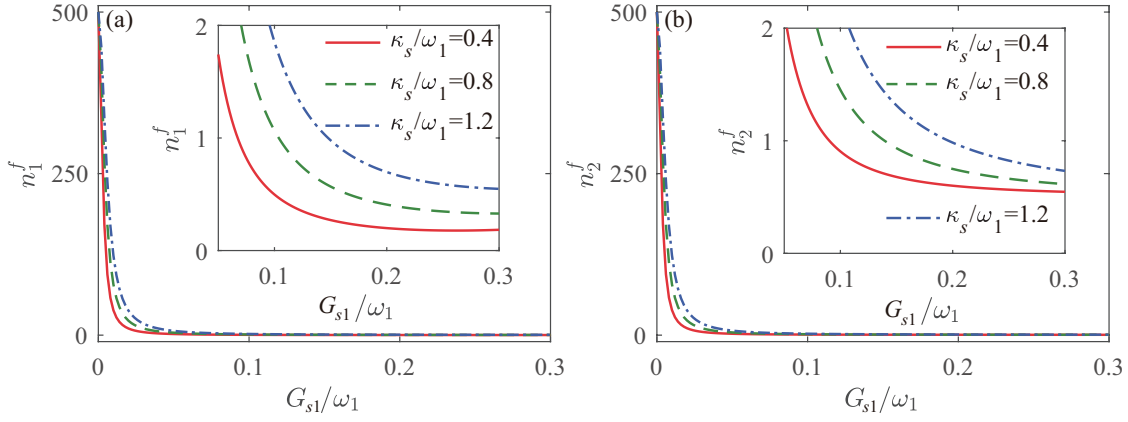


FIG. S3: The final mean phonon numbers (a)  $n_1^f$  and (b)  $n_2^f$  as functions of  $G_{s1}/\omega_1$  when the scaled cavity-field decay rate takes various values  $\kappa_s/\omega_1 = 0.4, 0.8$ , and  $1.2$ . Insets: Zoomed-in plots of the final mean phonon numbers as functions of  $G_{s1}/\omega_1$ , and the horizontal axis ranges from  $0.05$  to  $0.3$ . Other parameters used are  $\omega_2/\omega_1 = 1$ ,  $\Delta'_c/\omega_1 = \Delta'_s/\omega_1 = 1$ ,  $\kappa/\omega_1 = 0.1$ ,  $\gamma_1/\omega_1 = \gamma_2/\omega_1 = 10^{-5}$ ,  $G_1/\omega_1 = G_2/\omega_1 = 0.05$ , and  $\bar{n}_1 = \bar{n}_2 = 1000$ .

In the linearized optomechanical system, the covariance matrix  $\mathbf{V}$  satisfies the Lyapunov equation

$$\mathbf{A}\mathbf{V} + \mathbf{V}\mathbf{A}^T = -\mathbf{Q}. \quad (\text{S20})$$

Here, the matrix  $\mathbf{Q}$  is defined by

$$\mathbf{Q} = \frac{1}{2}(\mathbf{C} + \mathbf{C}^T), \quad (\text{S21})$$

where  $\mathbf{C}$  is the correlation matrix related to the noise operators. The matrix elements of  $\mathbf{C}$  are defined by

$$\langle \mathbf{N}_k(s) \mathbf{N}_l(s') \rangle = \mathbf{C}_{k,l} \delta(s - s'). \quad (\text{S22})$$

In this work, we consider the Markovian dissipation case, so the constant matrix  $\mathbf{C}$  can be obtained as

$$\mathbf{C} = \begin{pmatrix} 0 & 0 & 0 & 0 & 2\kappa & 0 & 0 & 0 \\ 0 & 0 & 0 & 0 & 0 & 2\kappa_s & 0 & 0 \\ 0 & 0 & 0 & 0 & 0 & 0 & 2\gamma_1(\bar{n}_1 + 1) & 0 \\ 0 & 0 & 0 & 0 & 0 & 0 & 0 & 2\gamma_2(\bar{n}_2 + 1) \\ 0 & 0 & 0 & 0 & 0 & 0 & 0 & 0 \\ 0 & 0 & 0 & 0 & 0 & 0 & 0 & 0 \\ 0 & 0 & 2\gamma_1\bar{n}_1 & 0 & 0 & 0 & 0 & 0 \\ 0 & 0 & 0 & 2\gamma_2\bar{n}_2 & 0 & 0 & 0 & 0 \end{pmatrix}. \quad (\text{S23})$$

By solving the Lyapunov equation, we obtain the covariance matrix  $\mathbf{V}$  defined in Eq. (S19), and then the final mean phonon numbers of the two mechanical modes can be obtained as

$$n_1^f = \langle \delta b_1^\dagger \delta b_1 \rangle = \mathbf{V}_{73} - \frac{1}{2}, \quad (\text{S24a})$$

$$n_2^f = \langle \delta b_2^\dagger \delta b_2 \rangle = \mathbf{V}_{84} - \frac{1}{2}, \quad (\text{S24b})$$

where  $\mathbf{V}_{73}$  and  $\mathbf{V}_{84}$  are the matrix elements of the covariance matrix  $\mathbf{V}$ .

Since the auxiliary cavity mode not only provides the direct channel to extract the thermal excitations from the mechanical mode  $b_1$ , but also provides a cooling channel to extract the thermal excitations from the mechanical mode  $b_2$ , the coupling strength  $G_{s1}$  between the auxiliary cavity mode  $a_s$  and the mechanical mode  $b_1$  is an important factor to the cooling efficiency.

To see this effect more clearly, in Figs. S3(a) and S3(b) we plot the final mean phonon numbers  $n_1^f$  and  $n_2^f$  as functions of the linearized optomechanical-coupling strength  $G_{s1}$  between the auxiliary cavity mode  $a_s$  and the mechanical mode  $b_1$  when the scaled cavity-field decay rate  $\kappa_s/\omega_1$  takes various values. Here, we see that the phonon numbers decrease with the increase of the coupling strength  $G_{s1}$ , which means that the increase of the coupling strength  $G_{s1}$  is beneficial to the ground-state cooling of the



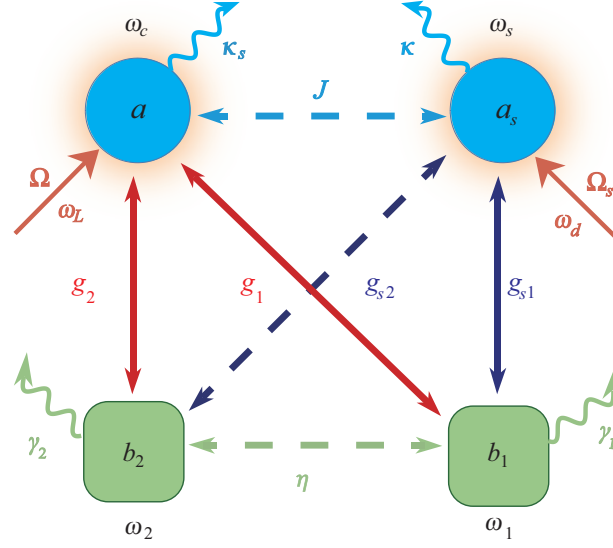


FIG. S4: Schematic of the network-coupled four-mode optomechanical system consisting of two cavity modes and two mechanical modes. In addition to the couplings and notations introduced in Fig. S1, here we introduce three new couplings: the phonon (photon)-hopping interaction with the coupling strength  $\eta$  ( $J$ ), the optomechanical-coupling strength  $g_{s2}$  between the auxiliary cavity mode  $a_s$  and the second mechanical mode  $b_2$ .

two mechanical modes. Moreover, the final mean phonon numbers are smaller for smaller values of the decay rate  $\kappa_{s1}/\omega_1$  under a certain parameter range, which is consistent with the analyses concerning the cooling efficiency on the sideband-resolution condition. We note that, in sideband cooling, the dependence of the cooling performance on the cavity-field decay rate is not a monotonous function relation. In particular, our simulations indicate that the final phonon numbers are smaller than one when the cavity-field decay rate  $\kappa_s$  is slightly larger than the mechanical resonance frequency  $\omega_1$ .

## S2. SIMULTANEOUS GROUND-STATE COOLING AND GENERAL DARK-MODE CONTROL IN THE NETWORK-COUPLED FOUR-MODE OPTOMECHANICAL SYSTEM

### A. Equations of motion and fourteen coupling configurations

In the above section we have shown that, by introducing an optomechanical coupling between the auxiliary cavity mode  $a_s$  and the mechanical mode  $b_1$ , the dark mode in this system can be broken and then the ground-state cooling of the two mechanical resonators can be realized. In practice, however, the diverse interactions among the degrees of freedom in this system are more complicated, so it is an interesting topic to study the general condition for breaking the dark-mode effect in a more general four-mode optomechanical system. In this section, we analyze the parameter conditions under which the dark mode is formed. We also study how to break the dark mode by controlling the couplings in the four-mode optomechanical system.

We now consider a network-coupled four-mode optomechanical system consisting of an intermediate coupling cavity mode and an auxiliary cavity mode, which are both coupled to the two mechanical modes via radiation-pressure interactions. Here, the two cavity (mechanical) modes are coupled to each other via a photon (phonon)-hopping interaction, as shown in Fig S4. In a rotating frame defined by the operator  $V(t) = \exp[-i(\omega_L a^\dagger a + \omega_d a_s^\dagger a_s)t]$  under  $\omega_L = \omega_d$ , the transformed Hamiltonian becomes

$$\begin{aligned}
 H_I = & \Delta_c a^\dagger a + \Delta_s a_s^\dagger a_s + J(a^\dagger a_s + a_s^\dagger a) + \eta(b_1^\dagger b_2 + b_2^\dagger b_1) \\
 & + \sum_{l=1,2} [\omega_l b_l^\dagger b_l + g_l a^\dagger a (b_l^\dagger + b_l) + g_{sl} a_s^\dagger a_s (b_l^\dagger + b_l)] \\
 & + (\Omega a^\dagger + \Omega_s a_s^\dagger + \text{H.c.}), \tag{S25}
 \end{aligned}$$

where some operators and variables have been defined in Eq. (S1). We also introduce the  $g_{s2}$  coupling term, the  $J$  coupling term, and the  $\eta$  coupling term, which correspond to the optomechanical coupling between modes  $a_s$  and  $b_2$ , the photon-hopping coupling, and the phonon-hopping coupling, respectively.

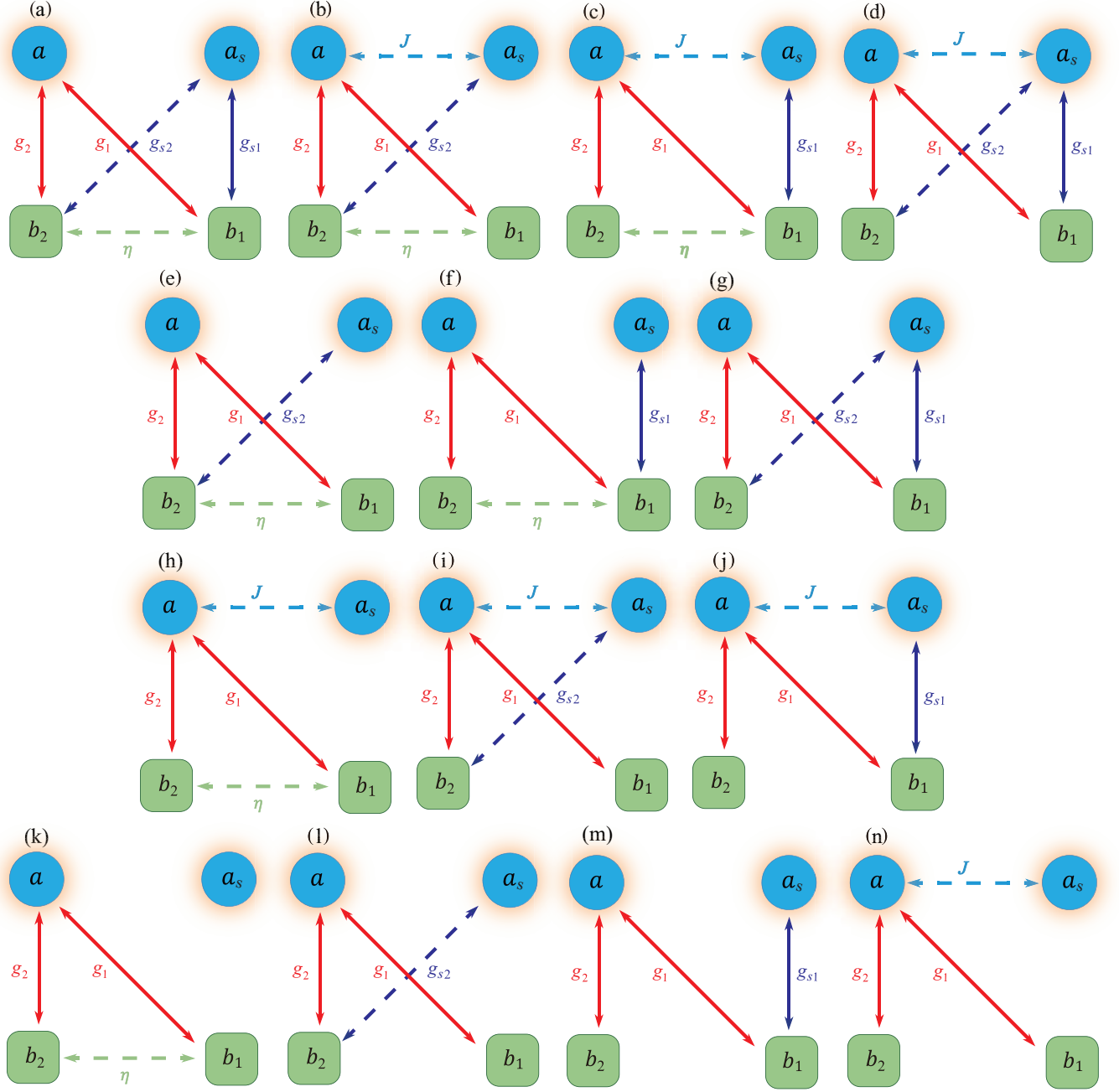


FIG. S5: Fourteen coupling configurations of the network-coupled four-mode optomechanical system, where  $J$ ,  $g_{l(l=1,2)}$  [ $g_{sl(l=1,2)}$ ], and  $\eta$  are the photon-hopping coupling strength, the optomechanical coupling strength between the intermediate (auxiliary) cavity mode and the  $l$ th mechanical mode, and the phonon-hopping coupling strength, respectively. Here, the two optomechanical couplings between the cavity mode  $a$  and the two mechanical modes  $b_1$  and  $b_2$  are kept, and the other couplings can be closed on demand. Then there are fourteen different coupling configurations. (a) The coupling channel  $J$  is closed ( $J = 0$ ). (b) The coupling channel  $g_{s1}$  is closed ( $g_{s1} = 0$ ). (c) The coupling channel  $g_{s2}$  is closed ( $g_{s2} = 0$ ). (d) The coupling channel  $\eta$  is closed ( $\eta = 0$ ). (e) The coupling channels  $J$  and  $g_{s1}$  are closed ( $J = g_{s1} = 0$ ). (f) The coupling channels  $J$  and  $g_{s2}$  are closed ( $J = g_{s2} = 0$ ). (g) The coupling channels  $J$  and  $\eta$  are closed ( $J = \eta = 0$ ). (h) The coupling channels  $g_{s1}$  and  $g_{s2}$  are closed ( $g_{s1} = g_{s2} = 0$ ). (i) The coupling channels  $g_{s1}$  and  $\eta$  are closed ( $g_{s1} = \eta = 0$ ). (j) The coupling channels  $g_{s2}$  and  $\eta$  are closed ( $g_{s2} = \eta = 0$ ). (k) The coupling channels  $J$ ,  $g_{s1}$ , and  $g_{s2}$  are closed ( $J = g_{s1} = g_{s2} = 0$ ). (l) The coupling channels  $J$ ,  $g_{s1}$ , and  $\eta$  are closed ( $J = g_{s1} = \eta = 0$ ). (m) The coupling channels  $J$ ,  $g_{s2}$ , and  $\eta$  are closed ( $J = g_{s2} = \eta = 0$ ). (n) The coupling channels  $g_{s1}$ ,  $g_{s2}$ , and  $\eta$  are closed ( $g_{s1} = g_{s2} = \eta = 0$ ). We point out that the single-photon optomechanical-coupling strengths  $g_1$ ,  $g_2$ ,  $g_{s1}$ , and  $g_{s2}$  are related to the linearized optomechanical-coupling strengths  $G_1$ ,  $G_2$ ,  $G_{s1}$ , and  $G_{s2}$  in the four-mode optomechanical system.

Based on the Hamiltonian (S25), we obtain the quantum Langevin equations for the system operators by phenomenologically adding the damping and noise terms into the Heisenberg equations. Following the similar linearization procedure as the one performed in Sec. S1, we obtain the linearized Langevin equations

$$\delta\dot{a} = -(\kappa + i\Delta'_c)\delta a - iJ\delta a_s - i \sum_{l=1,2} [G_l(\delta b_l + \delta b_l^\dagger)] + \sqrt{2\kappa}a_{\text{in}}, \quad (\text{S26a})$$

$$\delta\dot{a}_s = -(\kappa_s + i\Delta'_s)\delta a_s - iJ\delta a - i \sum_{l=1,2} [G_{sl}(\delta b_l + \delta b_l^\dagger)] + \sqrt{2\kappa_s}a_{s,\text{in}}, \quad (\text{S26b})$$

$$\delta\dot{b}_1 = -(i\omega_1 + \gamma_1)\delta b_1 - iG_1^*\delta a - iG_1\delta a^\dagger - iG_{s1}^*\delta a_s - iG_{s1}\delta a_s^\dagger - i\eta\delta b_2 + \sqrt{2\gamma_1}b_{1,\text{in}}, \quad (\text{S26c})$$

$$\delta\dot{b}_2 = -(i\omega_2 + \gamma_2)\delta b_2 - iG_2^*\delta a - iG_2\delta a^\dagger - iG_{s2}^*\delta a_s - iG_{s2}\delta a_s^\dagger - i\eta\delta b_1 + \sqrt{2\gamma_2}b_{2,\text{in}}, \quad (\text{S26d})$$

where  $\Delta'_s = \Delta_s + 2g_{s1}\text{Re}[\beta_1] + 2g_{s2}\text{Re}[\beta_2]$  is the renormalized driving detuning of the auxiliary cavity mode  $a_s$ . It should be pointed out that the parameter  $\Delta'_c$  and the linearized optomechanical-coupling strengths  $G_l$  and  $G_{sl(l=1,2)}$  have the same definition as those defined in Sec. S1. However, the coherent displacements of the steady state  $\alpha$ ,  $\alpha_s$ ,  $\beta_1$ , and  $\beta_2$  in the network-coupled four-mode optomechanical system should be replaced by the relations

$$\alpha \equiv \langle a \rangle_{\text{ss}} = \frac{-i(J\alpha_s + \Omega)}{\kappa + i\Delta'_c}, \quad (\text{S27a})$$

$$\alpha_s \equiv \langle a_s \rangle_{\text{ss}} = \frac{-i(J\alpha + \Omega_s)}{\kappa_s + i\Delta'_s}, \quad (\text{S27b})$$

$$\beta_1 \equiv \langle b_1 \rangle_{\text{ss}} = \frac{-i(\eta\beta_2 + g_1|\alpha|^2 + g_{s1}|\alpha_s|^2)}{\gamma_1 + i\omega_1}, \quad (\text{S27c})$$

$$\beta_2 \equiv \langle b_2 \rangle_{\text{ss}} = \frac{-i(\eta\beta_1 + g_2|\alpha|^2 + g_{s2}|\alpha_s|^2)}{\gamma_2 + i\omega_2}. \quad (\text{S27d})$$

For studying quantum cooling of the mechanical modes, we rewrite the linearized Langevin equations (S25) in a compact form  $\dot{\mathbf{u}}(t) = \mathbf{A}'\mathbf{u}(t) + \mathbf{N}(t)$ , where the form of the fluctuation operator vector  $\mathbf{u}(t)$  and the noise operator vector  $\mathbf{N}(t)$  is the same as those defined in Sec. S1 B, while the coefficient matrix  $\mathbf{A}'$  is given by

$$\mathbf{A}' = \begin{pmatrix} -(\kappa + i\Delta'_c) & -iJ & -iG_1 & -iG_2 & 0 & 0 & -iG_1 & -iG_2 \\ -iJ & -(i\Delta'_s + \kappa_s) & -iG_{s1} & -iG_{s2} & 0 & 0 & -iG_{s1} & -iG_{s2} \\ -iG_1^* & -iG_{s1}^* & -(i\omega_1 + \gamma_1) & -i\eta & -iG_1 & -iG_{s1} & 0 & 0 \\ -iG_2^* & -iG_{s2}^* & -i\eta & -(i\omega_2 + \gamma_2) & -iG_2 & -iG_{s2} & 0 & 0 \\ 0 & 0 & iG_1^* & iG_2^* & -(\kappa - i\Delta'_c) & iJ & iG_1^* & iG_2^* \\ 0 & 0 & iG_{s1}^* & iG_{s2}^* & iJ & -(\kappa_s - i\Delta'_s) & iG_{s1}^* & iG_{s2}^* \\ iG_1^* & iG_{s1}^* & 0 & 0 & iG_1 & iG_{s1} & -(\gamma_1 - i\omega_1) & i\eta \\ iG_2^* & iG_{s2}^* & 0 & 0 & iG_2 & iG_{s2} & i\eta & -(\gamma_2 - i\omega_2) \end{pmatrix}. \quad (\text{S28})$$

Following the same procedure as the one performed in Sec. S1 C, we can also obtain the steady-state expression of the covariance matrix  $\mathbf{V}'$ , which is defined by  $\mathbf{A}'\mathbf{V}' + \mathbf{V}'\mathbf{A}'^T = -\mathbf{Q}$ , where  $\mathbf{Q}$  is given by Eq. (S21). Then the final mean phonon numbers in the two mechanical resonators can be obtained.

To clearly analyze the influence of these couplings in the four-mode optomechanical system on the ground-state cooling, below we consider various cases of different coupling configurations, as shown in Fig. S5. To analyze that the dark-mode effect in this system when the frequencies of the two mechanical modes are degenerate, we consider the case where the two coupling channels  $g_1$  and  $g_2$  always exist. Then we study various cases of coupling configurations by controlling the four coupling channels  $J$ ,  $g_{s1}$ ,  $g_{s2}$ , and  $\eta$ . In Figs. S5(a)-S5(d) and Figs. S5(e)-S5(j), we show that one or two coupling channels of  $J$ ,  $g_{s1}$ ,  $g_{s2}$ , and  $\eta$  are closed, respectively. While in Figs. S5(k)-S5(n), three of the four coupling channels  $J$ ,  $g_{s1}$ ,  $g_{s2}$ , and  $\eta$  are closed. Therefore, when the coupling channels  $g_1$  and  $g_2$  remain, there are fourteen cases of coupling configurations, as shown in Fig. S5.

## B. Cooling performance corresponding to the fourteen coupling configurations

Corresponding to the fourteen cases depicted in Fig. S5, the final mean phonon numbers  $n_1^f$  and  $n_2^f$  versus the scaled cavity-field decay rate  $\kappa/\omega_1$  have been presented in Fig. 4 in the main text. To clearly know the coupling configurations for the ground-state cooling, in Table I, we present the cooling performance of these mechanical modes corresponding to the fourteen coupling configurations. We also list the results of the two parameter conditions  $K_1$  and  $K_2$  defined in Eqs. (S36), and the ground-state

TABLE I: The cooling performance of the two degenerate mechanical modes corresponding to the fourteen coupling configurations. We also present the parameter conditions for the appearance of the dark mode, the ground-state cooling results, and the dark-mode breaking results.

	Coupling closed	Values of $K_1$ and $K_2$	Ground state cooling	Dark mode breaking	Corresponding to the panel in Fig. S5
One coupling is closed	$J = 0, G_1 = G_2,$ $G_{s1} = G_{s2},$ and $\eta \neq 0.$	$K_1 = 0, K_2 = 0.$	No	No	(a)
	$G_{s1} = 0, G_1 = G_2,$ $J \neq 0, G_{s2} \neq 0,$ and $\eta \neq 0.$	$K_1 = 0, K_2 \neq 0.$	Yes	Yes	(b)
	$G_{s2} = 0, G_1 = G_2,$ $J \neq 0, G_{s1} \neq 0,$ and $\eta \neq 0.$	$K_1 = 0, K_2 \neq 0.$	Yes	Yes	(c)
	$\eta = 0, G_1 = G_2,$ $G_{s1} = G_{s2},$ and $J \neq 0.$	$K_1 = 0, K_2 = 0.$	No	No	(d)
Two couplings are closed	$J = G_{s1} = 0, G_1 = G_2,$ $G_{s2} \neq 0,$ and $\eta \neq 0.$	$K_1 = 0, K_2 \neq 0.$	Yes	Yes	(e)
	$J = G_{s2} = 0, G_1 = G_2,$ $G_{s1} \neq 0,$ and $\eta \neq 0.$	$K_1 = 0, K_2 \neq 0.$	Yes	Yes	(f)
	$J = \eta = 0, G_1 = G_2,$ and $G_{s1} = G_{s2}.$	$K_1 = 0, K_2 = 0.$	No	No	(g)
	$G_{s1} = G_{s2} = 0, G_1 = G_2,$ $J \neq 0,$ and $\eta \neq 0.$	$K_1 = 0, K_2 = 0.$	No	No	(h)
	$G_{s1} = \eta = 0, G_1 = G_2,$ $J \neq 0,$ and $G_{s2} \neq 0.$	$K_1 = 0, K_2 \neq 0.$	Yes	Yes	(i)
	$G_{s2} = \eta = 0, G_1 = G_2,$ $J \neq 0,$ and $G_{s1} \neq 0.$	$K_1 = 0, K_2 \neq 0.$	Yes	Yes	(j)
Three couplings are closed	$J = G_{s1} = G_{s2} = 0,$ $G_1 = G_2,$ and $\eta \neq 0.$	$K_1 = 0, K_2 = 0.$	No	No	(k)
	$J = G_{s1} = \eta = 0,$ $G_1 = G_2,$ and $G_{s2} \neq 0.$	$K_1 = 0, K_2 \neq 0.$	Yes	Yes	(l)
	$J = G_{s2} = \eta = 0,$ $G_1 = G_2,$ and $G_{s1} \neq 0.$	$K_1 = 0, K_2 \neq 0.$	Yes	Yes	(m)
	$G_{s1} = G_{s2} = \eta = 0,$ $G_1 = G_2,$ and $J \neq 0.$	$K_1 = 0, K_2 = 0.$	No	No	(n)

cooling results. Based on Table I, we know the coupling configuration for ground-state cooling of the two mechanical modes in the network-coupled four-mode optomechanical system. The physical mechanism for these results can also be explained clearly based on the analytical parameter conditions.

Based on the above discussions, we find that  $G_{s1}$  and  $G_{s2}$  play an important role in the breaking of the dark mode in this system. Only when one of  $G_{s1}$  and  $G_{s2}$  is closed, the dark mode can be broken. When both or neither of  $G_{s1}$  and  $G_{s2}$  are closed, the dark mode cannot be broken. In particular, the breaking of the dark mode is independent of both the photon and phonon coupling channels.

In order to better understand the influence of the linearized optomechanical-coupling strengths  $G_{s1}$  and  $G_{s2}$  on the final mean phonon numbers, in Fig. S6(a), we plot the final mean phonon numbers  $n_1^f$  and  $n_2^f$  as functions of the scaled decay rate  $\kappa/\omega_1$  when the linearized optomechanical-coupling strengths take the values  $G_{s2}/\omega_1 = 4G_{s1}/\omega_1 = 0.08$  and  $G_{s1}/\omega_1 = 4G_{s2}/\omega_1 = 0.08$ . Here we can see that the ground-state cooling of the two mechanical modes can be realized in the resolved-sideband regime. Besides, the values of  $n_1^f$  and  $n_2^f$  are approximately exchanged in these two cases, and this is because the parameters of  $G_{s1}$  and  $G_{s2}$  in these two cases are just antisymmetric. In Fig. S6(b), we plot the final mean phonon numbers  $n_1^f$  and  $n_2^f$  as functions of the ratio  $G_{s2}/G_{s1}$  when the linearized optomechanical-coupling strength  $G_{s1}/\omega_1 = 0.08$ . When  $G_{s2}/G_{s1} \leq 1$  ( $G_{s2}/G_{s1} \geq 1$ ), the final mean phonon numbers of the two mechanical modes increase (decrease) when increasing the ratio  $G_{s2}/G_{s1}$ , i.e., the cooling performance of the two resonators is exchanged at the point  $G_{s2}/G_{s1} = 1$ . Due to the dark-mode effect, the ground-state cooling of the two mechanical resonators is unfeasible for finite values of the ratio  $G_{s2}/G_{s1}$ . In this case, the ground-state cooling can be realized by choosing  $G_{s2}/G_{s1} < 0.4$ .

The photon (phonon)-hopping coupling strength also has a great influence on the ground-state cooling of the mechanical modes. Below we investigate the dependence of the cooling performance on the photon (phonon)-hopping interaction between



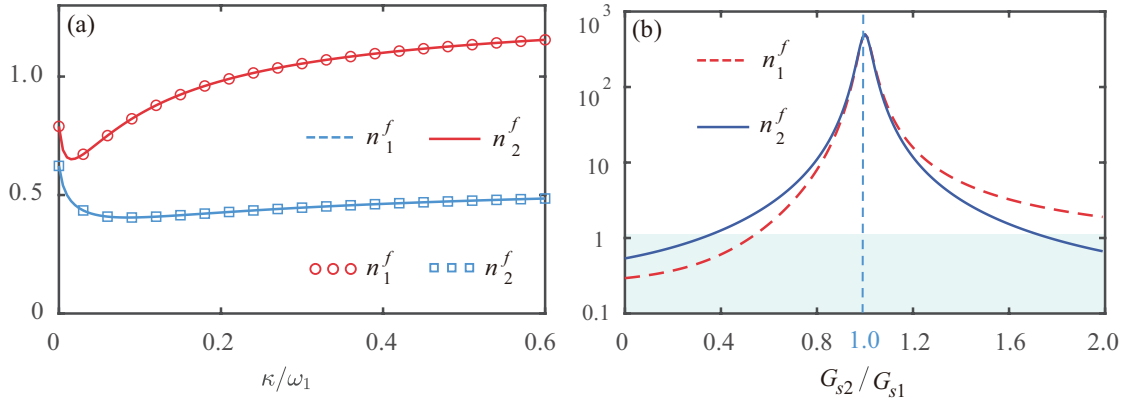


FIG. S6: (a) The final mean phonon numbers  $n_1^f$  and  $n_2^f$  versus the scaled cavity-field decay rate  $\kappa/\omega_1$  when  $G_{s2}/\omega_1 = 4G_{s1}/\omega_1 = 0.08$  (dashed blue curve and solid red curve) and  $G_{s1}/\omega_1 = 4G_{s2}/\omega_1 = 0.08$  (red circle and blue rectangle). (b) The final mean phonon numbers  $n_1^f$  (solid blue curves) and  $n_2^f$  (dashed red curves) versus the ratio  $G_{s2}/G_{s1}$  when the linearized optomechanical coupling strength  $G_{s1}/\omega_1 = 0.08$ . Other parameters used in this system are  $\omega_2/\omega_1 = 1$ ,  $\gamma_1/\omega_1 = \gamma_2/\omega_1 = 10^{-5}$ ,  $\kappa/\omega_1 = \kappa_s/\omega_1 = 0.1$ ,  $J/\omega_1 = \eta/\omega_1 = 0.03$ ,  $\Delta'_c/\omega_1 = \Delta'_s/\omega_1 = 1$ ,  $G_1/\omega_1 = G_2/\omega_1 = 0.05$ , and  $\bar{n}_1 = \bar{n}_2 = 1000$ .

the two (cavity) mechanical modes. In Fig. S7, we plot the phonon numbers  $n_1^f$  and  $n_2^f$  as functions of the decay rate  $\kappa/\omega_1$ , when the scaled photon (phonon)-hopping coupling strength takes various values. Here, we see from Figs. S7(a) and S7(c) that the phonon numbers increase when increasing the coupling strength  $J$ , which means that the increase of the coupling strength  $J$  is harmful to the ground-state cooling of the two mechanical modes. From Figs. S7(b) and S7(d) we can see that the cooling efficiency of the mechanical mode  $b_1$  is better for a smaller value of the phonon-hopping coupling strength  $\eta$ . However, for the second mechanical mode  $b_2$ , the dependence of its cooling efficiency on the coupling strength  $\eta$  is not a monotonous relation for larger values of the decay rate  $\kappa/\omega_1$ . This is because the first resonator provides a new cooling channel for the second resonator, then its thermal excitations are extracted by the auxiliary cavity mode. However, the second resonator will encumber the cooling efficiency of the first resonator, so the phonon number  $n_1^f$  increases.

### C. General parameter conditions for forming and breaking the dark mode

In this subsection, we analyze the parameter conditions under which the dark mode is formed in the network-coupled optomechanical system. We also study the method for breaking the dark-mode effect. Based on Eq. (S26), we can derive the approximate linearized Hamiltonian, which governs the dynamics of the system. For implementing the cooling scheme, the system should work in the red-sideband resonance regime, in which the rotating-wave approximation can be safely performed. By discarding the noise terms, the linearized optomechanical Hamiltonian can be written as

$$H_{\text{RWA}} = \Delta'_c \delta a^\dagger \delta a + \Delta'_s \delta a_s^\dagger \delta a_s + J(\delta a^\dagger \delta a_s + \delta a_s^\dagger \delta a) + \eta(\delta b_1^\dagger \delta b_2 + \delta b_2^\dagger \delta b_1) + \sum_{l=1,2} [\omega_l \delta b_l^\dagger \delta b_l + G_l(\delta a \delta b_l^\dagger + \delta a^\dagger \delta b_l) + G_{sl}(\delta a_s \delta b_l^\dagger + \delta a_s^\dagger \delta b_l)], \quad (\text{S29})$$

where these parameters have been introduced in Eq. (S26).

To clearly see the dark-mode effect in this network-coupled optomechanical system, we first consider the case where the auxiliary cavity is absent, i.e.,  $\Delta'_s = 0$ ,  $J = 0$ , and  $G_{sl} = 0$ , then Hamiltonian (S29) becomes

$$\tilde{H}_{\text{RWA}} = \Delta'_c \delta a^\dagger \delta a + \eta(\delta b_1^\dagger \delta b_2 + \delta b_2^\dagger \delta b_1) + \sum_{l=1,2} [\omega_l \delta b_l^\dagger \delta b_l + G_l(\delta a \delta b_l^\dagger + \delta a^\dagger \delta b_l)]. \quad (\text{S30})$$

In particular, we introduce two hybrid mechanical modes  $B_+$  and  $B_-$  as

$$B_+ = \frac{1}{\sqrt{G_1^2 + G_2^2}}(G_1 \delta b_1 + G_2 \delta b_2), \quad (\text{S31a})$$

$$B_- = \frac{1}{\sqrt{G_1^2 + G_2^2}}(G_2 \delta b_1 - G_1 \delta b_2). \quad (\text{S31b})$$

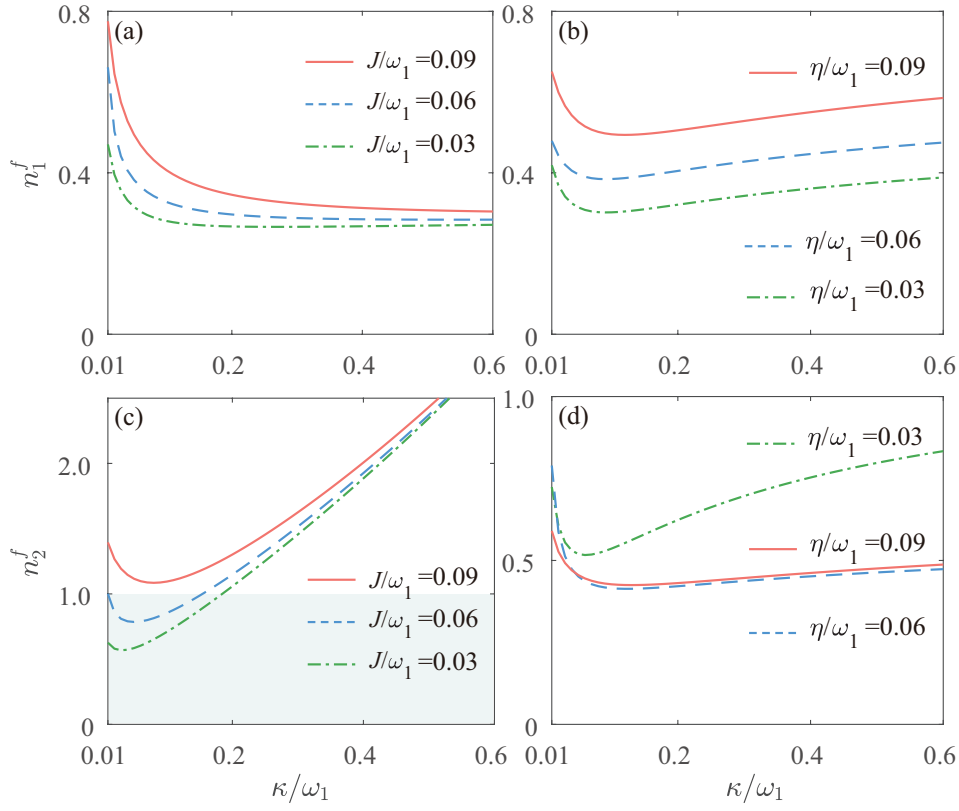


FIG. S7: The final mean phonon numbers (a) [(c)]  $n_1^f$  and (b) [(d)]  $n_2^f$  as functions of the cavity decay rate  $\kappa/\omega_1$  when the scaled photon (phonon)-hopping coupling strength takes various values  $J/\omega_1$  ( $\eta/\omega_1$ ) = 0.03, 0.06, and 0.09. Other parameters used are  $\omega_2/\omega_1 = 1$ ,  $\Delta'_c/\omega_1 = \Delta'_s/\omega_1 = 1$ ,  $\kappa_s/\omega_1 = 0.1$ ,  $\gamma_1/\omega_1 = \gamma_2/\omega_1 = 10^{-5}$ ,  $G_1/\omega_1 = G_2/\omega_1 = 0.05$ ,  $G_{s1}/\omega_1 = 0.08$ , and  $\bar{n}_1 = \bar{n}_2 = 1000$ .

Here, the new operators satisfy the bosonic commutation relations  $[B_+, B_+^\dagger] = 1$  and  $[B_-, B_-^\dagger] = 1$ . By substituting operators  $B_+$  ( $B_+^\dagger$ ) and  $B_-$  ( $B_-^\dagger$ ) into Eq. (S30), the Hamiltonian  $\tilde{H}_{\text{RWA}}$  can be re-expressed as

$$\tilde{H}_{\text{RWA}} = \Delta'_c \delta a^\dagger \delta a + \omega_+ B_+^\dagger B_+ + \omega_- B_-^\dagger B_- + G_+ (\delta a B_+^\dagger + B_+ \delta a^\dagger) + \zeta (B_+^\dagger B_- + B_-^\dagger B_+), \quad (\text{S32})$$

where  $\omega_\pm$  are the resonance frequencies of the two hybrid modes,  $\zeta$  and  $G_+$  are the coupling strengths, which are defined by

$$\omega_+ = \frac{\omega_1 G_1^2 + \omega_2 G_2^2 + 2\eta G_1 G_2}{G_1^2 + G_2^2}, \quad (\text{S33a})$$

$$\omega_- = \frac{\omega_1 G_2^2 + \omega_2 G_1^2 - 2\eta G_1 G_2}{G_1^2 + G_2^2}, \quad (\text{S33b})$$

$$G_+ = \sqrt{G_1^2 + G_2^2}, \quad (\text{S33c})$$

$$\zeta = \frac{(\omega_1 - \omega_2) G_1 G_2 + \eta (G_2^2 - G_1^2)}{G_1^2 + G_2^2}. \quad (\text{S33d})$$

From Eq. (S33) we can see that the two hybrid modes  $B_-$  and  $B_+$  are decoupled from each other ( $\zeta = 0$ ) when  $\omega_1 = \omega_2$  and  $\eta = 0$ . Moreover, the hybrid mode  $B_-$  also decouples from the cavity mode  $a$ , which means that the hybrid mode  $B_-$  becomes a dark mode. At this time, the ground-state cooling of the two mechanical modes is largely suppressed, which is consistent with the numerical results. When  $\omega_1 = \omega_2$  and  $G_1 \neq G_2$ , the dark mode can be broken by coupling two mechanical modes together to form a loop-coupled configuration ( $\eta \neq 0$ ). However, when the coupling strengths  $G_1 = G_2$ , the dark mode cannot be broken even if a loop-coupled optomechanical system is formed ( $\eta \neq 0$  and  $\zeta = 0$ ).

To break the dark-mode effect in this optomechanical system, we introduce an auxiliary cavity mode, which is coupled to two mechanical modes via the radiation-pressure interaction. By substituting operators  $B_+$  ( $B_+^\dagger$ ) and  $B_-$  ( $B_-^\dagger$ ) into Eq. (S29), the

Hamiltonian  $H_{\text{RWA}}$  given in Eq. (S29) becomes

$$H_{\text{RWA}} = \Delta'_c \delta a^\dagger \delta a + \Delta'_s \delta a_s^\dagger \delta a_s + J(\delta a^\dagger \delta a_s + \delta a_s^\dagger \delta a) + \omega_+ B_+^\dagger B_+ + \omega_- B_-^\dagger B_- + \zeta(B_+^\dagger B_- + B_-^\dagger B_+) \\ + G_+(\delta a B_+^\dagger + B_+ \delta a^\dagger) + G_{s+}(\delta a_s B_+^\dagger + \delta a_s^\dagger B_+) + G_{s-}(\delta a_s B_-^\dagger + \delta a_s^\dagger B_-), \quad (\text{S34})$$

where we introduce two new coupling strengths  $G_{s+}$  and  $G_{s-}$ ,

$$G_{s+} = \frac{G_{s1}G_1 + G_{s2}G_2}{\sqrt{G_1^2 + G_2^2}}, \quad (\text{S35a})$$

$$G_{s-} = \frac{G_{s1}G_2 - G_{s2}G_1}{\sqrt{G_1^2 + G_2^2}}. \quad (\text{S35b})$$

Here, we can see that the mode  $B_+$  always couples with the auxiliary cavity mode  $a_s$  because  $G_{s+} > 0$  when the two couplings  $G_{s1}$  and  $G_{s2}$  do not disappear at the same time, given that  $G_1$  and  $G_2$  always exist. Then the parameter conditions for the appearance of a dark mode ( $B_-$ , decoupling from the two modes  $B_+$  and  $\delta a_s$ ) are  $\zeta = 0$  and  $G_{s-} = 0$ . If we introduce two variables as

$$K_1 = (\omega_1 - \omega_2)G_1G_2 + \eta(G_2^2 - G_1^2), \quad (\text{S36a})$$

$$K_2 = G_{s1}G_2 - G_{s2}G_1. \quad (\text{S36b})$$

Then the parameter conditions for the appearance of the dark mode is

$$K_1 = 0, \quad (\text{S37a})$$

$$K_2 = 0. \quad (\text{S37b})$$

Therefore, the general dark-mode-breaking condition is that both  $\zeta$  and  $G_{s-}$  cannot be zero at the same time.

In the following we analyze various cases in which the dark mode appears or disappears in the degenerate-resonator case ( $\omega_1 = \omega_2$ ).

(i) In the case of  $\eta = 0$ , i.e.,  $\zeta = 0$ . It can be seen from Eq. (S35) that when  $G_{s1}G_2 - G_{s2}G_1 = 0$  ( $G_{s1}/G_{s2} = G_1/G_2$ ), the hybrid mechanical mode  $B_-$  (the dark mode) decouples from both the cavity mode  $a$  and the auxiliary cavity mode  $a_s$ . In this situation, the phonon excitations stored in the dark mode cannot be extracted through the cooling channel. In this case, the parameter  $J$  has no effect on the breaking of the dark-mode effect. These analyses are consistent with the results obtained by numerically calculations.

(ii) In the case of  $\eta \neq 0$  and  $G_1 \neq G_2$ , i.e.,  $\zeta \neq 0$ . we can find that the dark mode can be broken regardless of whether the auxiliary cavity mode appears or not (namely, there is no dark mode).

(iii) In the case of  $\eta \neq 0$  and  $G_1 = G_2$ , i.e.,  $\zeta = 0$ , there are two different situations. First, in the case of symmetric coupling ( $G_{s1} = G_{s2}$ ), we can see from Eq. (S35) that  $G_{s-} = 0$ . At this time, the hybrid mechanical mode  $B_-$  decouples from both the cavity mode  $a$  and the auxiliary cavity mode  $a_s$ , i.e.,  $B_-$  becomes a dark mode. However, in the case of asymmetric coupling ( $G_{s1} \neq G_{s2}$ ), i.e.,  $G_{s-} \neq 0$ , we can see that the two hybrid mechanical modes  $B_-$  and  $B_+$  are coupled with the auxiliary cavity mode  $a_s$ . Even if the hybrid mode  $B_-$  is decoupled from both the cavity mode  $a$  and the hybrid mode  $B_+$  at the same time, the ground-state cooling of the two mechanical resonators becomes accessible through the cooling channel associated with the auxiliary cavity mode  $a_s$ . Obviously, when one of the two coupling strengths  $G_{s1}$  and  $G_{s2}$  is 0, the dark-mode effect can be naturally broken. These analyses are consistent with the cooling results in the fourteen cases. Generally speaking, to break the dark mode formed in a three-mode optomechanical system consisting of a cavity mode and two mechanical modes, the easiest way is to introduce an auxiliary cavity mode to couple with one of the two mechanical modes.

### S3. SIMULTANEOUS GROUND-STATE COOLING AND DARK-MODE BREAKING IN A MULTIPLE-MECHANICAL-MODE OPTOMECHANICAL SYSTEM

In this section, we study the simultaneous ground-state cooling of  $N$  mechanical modes in a multiple-mechanical-mode optomechanical system, in which an intermediate cavity mode is coupled to  $N$  ( $N \geq 3$ ) mechanical modes [see Fig. S8(a)]. To implement the simultaneous ground-state cooling, we introduce an auxiliary cavity mode coupled to the first mechanical mode. We also introduce the phonon-hopping coupling between all the neighboring two mechanical modes [see Fig. S8(b)]. We also analyze the parameter conditions for forming the dark mode and for breaking the dark modes.

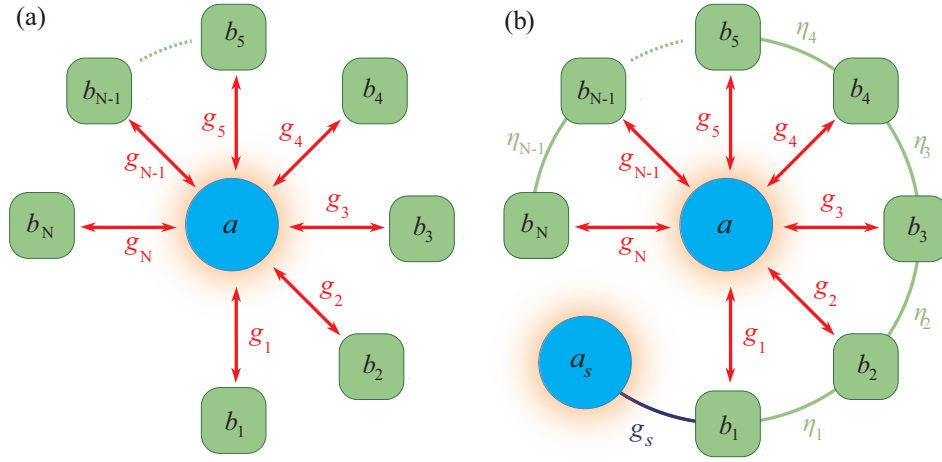


FIG. S8: (a) The  $N$ -mechanical-mode optomechanical system: a cavity-field mode simultaneously couples to  $N$  mechanical modes through the optomechanical interactions. (b) The optomechanical interaction between an auxiliary cavity mode and the mechanical mode  $b_1$ , the phonon-hopping interactions between two neighboring mechanical modes are introduced into the  $N$ -mechanical-mode optomechanical system described by panel (a). Note that there is no direct coupling between the first mechanical mode and the  $N$ th mechanical mode.

### A. Simultaneous ground-state cooling of $N$ mechanical modes

We consider a multiple-mechanical-mode optomechanical system, which consists of an intermediate cavity mode, an auxiliary cavity mode, and  $N$  ( $N \geq 3$ ) mechanical resonators [see Fig. S8(b)]. In a rotating frame defined by the transformation operator  $\exp[-i(\omega_L a^\dagger a + \omega_d a_s^\dagger a_s)t]$ , the Hamiltonian of this system is written as

$$\begin{aligned}
 H_I = & \Delta_c a^\dagger a + \sum_{l=1}^N [\omega_l b_l^\dagger b_l + g_l a^\dagger a (b_l^\dagger + b_l)] + \sum_{l=1}^{N-1} \eta_l (b_l^\dagger b_{l+1} + b_{l+1}^\dagger b_l) + (\Omega a^\dagger + \text{H.c.}) \\
 & + \Delta_s a_s^\dagger a_s + g_s a_s^\dagger a_s (b_1^\dagger + b_1) + (\Omega_s a_s^\dagger + \text{H.c.}),
 \end{aligned} \tag{S38}$$

where  $\Delta_c = \omega_c - \omega_L$  ( $\Delta_s = \omega_s - \omega_d$ ) is the detuning of the cavity-field frequency  $\omega_c$  ( $\omega_s$ ) with respect to the driving frequency  $\omega_L$  ( $\omega_d$ ). The operators  $a$  ( $a^\dagger$ ),  $a_s$  ( $a_s^\dagger$ ), and  $b_l$  ( $b_l^\dagger$ ) are, respectively, the annihilation (creation) operators of the cavity-field mode, the auxiliary cavity mode and the  $l$ th mechanical resonator (with the resonance frequency  $\omega_l$ ). The optomechanical interactions between the cavity mode (auxiliary cavity mode) and the  $l$ th mechanical resonator are described by the  $g_l$  ( $g_s$ ) terms. The cavity-field driving is denoted by the  $\Omega$  term (with  $\Omega$  being the driving amplitude). The parameters  $\omega_L$  ( $\omega_d$ ) and  $\Omega$  ( $\Omega_s$ ) are the driving frequency and amplitude associated with the driving field of the cavity mode  $a$  ( $a_s$ ), respectively. Based on the Hamiltonian in Eq. (S38), the quantum Langevin equations of this system can be obtained by phenomenologically adding the damping and noise terms into the Heisenberg equations as

$$\begin{aligned}
 \dot{a} &= -i\Delta_c a - i[g_1 a(b_1 + b_1^\dagger) + g_2 a(b_2 + b_2^\dagger) + \dots + g_N a(b_N^\dagger + b_N)] - i\Omega - \kappa a + \sqrt{2\kappa} a_{\text{in}}, \\
 \dot{a}_s &= -i[\Delta_s a_s + g_s a_s(b_1^\dagger + b_1) + \Omega_s] - \kappa_s a_s + \sqrt{2\kappa_s} a_{s,\text{in}}, \\
 \dot{b}_1 &= -i(\omega_1 b_1 + g_1 a^\dagger a + g_s a_s^\dagger a_s + \eta_1 b_2) - \gamma_1 b_1 + \sqrt{2\gamma_1} b_{1,\text{in}}, \\
 \dot{b}_2 &= -i(\omega_2 b_2 + g_2 a^\dagger a + \eta_1 b_1 + \eta_2 b_3) - \gamma_2 b_2 + \sqrt{2\gamma_2} b_{2,\text{in}}, \\
 \dot{b}_3 &= -i(\omega_3 b_3 + g_3 a^\dagger a + \eta_2 b_2 + \eta_3 b_4) - \gamma_3 b_3 + \sqrt{2\gamma_3} b_{3,\text{in}}, \\
 &\vdots \\
 \dot{b}_{N-1} &= -i(\omega_{N-1} b_{N-1} + g_{N-1} a^\dagger a + \eta_{N-2} b_{N-2} + \eta_{N-1} b_N) - \gamma_{N-1} b_{N-1} + \sqrt{2\gamma_{N-1}} b_{N-1,\text{in}}, \\
 \dot{b}_N &= -i(\omega_N b_N + g_N a^\dagger a + \eta_{N-1} b_{N-1}) - \gamma_N b_N + \sqrt{2\gamma_N} b_{N,\text{in}},
 \end{aligned} \tag{S39}$$

Similar to the two-mechanical-mode case, we consider the strong-driving regime of the cavity fields such that the average photon numbers in the cavities are large enough and then the linearization procedure can be used to simplify the physical model. By expressing the operators in Eq. (S39) as the sum of their steady-state mean values and quantum fluctuations, (i.e.,



$o = \langle o \rangle_{ss} + \delta o$  for operators  $a$ ,  $a^\dagger$ ,  $a_s$ ,  $a_s^\dagger$ ,  $b_{l=1-N}$ , and  $b_l^\dagger$ . then we obtain the linearized equations of motion for the quantum fluctuations

$$\begin{aligned}
\delta \dot{a} &= -(\kappa + i\Delta'_c)\delta a - i[g_1\alpha(\delta b_1 + \delta b_1^\dagger) + g_2\alpha(\delta b_2 + \delta b_2^\dagger) + \dots + ig_N\alpha(\delta b_N + \delta b_N^\dagger)] + \sqrt{2\kappa}a_{\text{in}}, \\
\delta \dot{a}_s &= -(\kappa_s + i\Delta'_s)\delta a_s - ig_s\alpha_s(\delta b_1 + \delta b_1^\dagger) + \sqrt{2\kappa_{s1}}a_{s1,\text{in}}, \\
\delta \dot{b}_1 &= -(\gamma_1 + i\omega_1)\delta b_1 - ig_1\alpha^*\delta a - ig_1\alpha\delta a^\dagger - ig_s\alpha_s^*\delta a_s - ig_s\alpha_s\delta a_s^\dagger - i\eta_1\delta b_2 + \sqrt{2\gamma_1}b_{1,\text{in}}, \\
\delta \dot{b}_2 &= -(\gamma_2 + i\omega_2)\delta b_2 - ig_2\alpha^*\delta a - ig_2\alpha\delta a^\dagger - i\eta_1\delta b_1 - i\eta_2\delta b_3 + \sqrt{2\gamma_2}b_{2,\text{in}}, \\
\delta \dot{b}_3 &= -(\gamma_3 + i\omega_3)\delta b_3 - ig_3\alpha^*\delta a - ig_3\alpha\delta a^\dagger - i\eta_2\delta b_2 - i\eta_3\delta b_4 + \sqrt{2\gamma_3}b_{3,\text{in}}, \\
&\vdots \\
\delta \dot{b}_{N-1} &= -(\gamma_{N-1} + i\omega_{N-1})\delta b_{N-1} - ig_{N-1}\alpha^*\delta a - ig_{N-1}\alpha\delta a^\dagger - i\eta_{N-2}\delta b_{N-2} \\
&\quad - i\eta_{N-1}\delta b_N + \sqrt{2\gamma_{N-1}}b_{N-1,\text{in}}, \\
\delta \dot{b}_N &= -(\gamma_N + i\omega_N)\delta b_N - ig_N\alpha^*\delta a - ig_N\alpha\delta a^\dagger - i\eta_{N-1}\delta b_{N-1} + \sqrt{2\gamma_N}b_{N,\text{in}}
\end{aligned} \tag{S40}$$

where  $\Delta'_c = \Delta_c + \sum_{l=1}^N g_l(\beta_l + \beta_l^*)$  [ $\Delta'_s = \Delta_s + g_s(\beta_1 + \beta_1^*)$ ] is the normalized driving detuning of the cavity mode  $a$  ( $a_s$ ), and  $G_l = g_l|\alpha|$  ( $G_s = g_s|\alpha_s|$ ) is the linearized optomechanical-coupling strength between the cavity mode  $a$  ( $a_s$ ) and the  $l$ th mechanical mode (mechanical mode  $b_1$ ).

We study the simultaneous ground state cooling of multiple mechanical modes in the  $N$ -mechanical-mode optomechanical system. To evaluate the cooling performance of the multiple mechanical modes, we calculate the final mean phonon numbers in these mechanical modes. Therefore, we now rewrite the linearized quantum Langevin equations (S40) as

$$\dot{\tilde{\mathbf{u}}}(t) = \tilde{\mathbf{A}}\tilde{\mathbf{u}}(t) + \tilde{\mathbf{N}}(t), \tag{S41}$$

where we introduce the vectors of the system operators

$$\tilde{\mathbf{u}}(t) = [\delta a(t), \delta a_s(t), \delta b_1(t), \dots, \delta b_{N-1}(t), \delta b_N(t), \delta a^\dagger(t), \delta a_s^\dagger(t), \delta b_1^\dagger(t), \dots, \delta b_{N-1}^\dagger(t), \delta b_N^\dagger(t)]^T, \tag{S42}$$

the vector of the noise operators

$$\begin{aligned}
\tilde{\mathbf{N}}(t) &= \sqrt{2} \left[ \sqrt{\kappa}a_{\text{in}}(t), \sqrt{\kappa_s}a_{s,\text{in}}(t), \sqrt{\gamma_1}b_{1,\text{in}}(t), \dots, \sqrt{\gamma_{N-1}}b_{N-1,\text{in}}(t), \sqrt{\gamma_N}b_{N,\text{in}}(t), \right. \\
&\quad \left. \sqrt{\kappa}a_{\text{in}}^\dagger(t), \sqrt{\kappa_s}a_{s,\text{in}}^\dagger(t), \sqrt{\gamma_1}b_{1,\text{in}}^\dagger(t), \dots, \sqrt{\gamma_{N-1}}b_{N-1,\text{in}}^\dagger(t), \sqrt{\gamma_N}b_{N,\text{in}}^\dagger(t) \right]^T,
\end{aligned} \tag{S43}$$

and the coefficient matrix  $\tilde{\mathbf{A}} = \begin{pmatrix} \mathbf{P} & \mathbf{R} \\ \mathbf{R}^* & \mathbf{P}^* \end{pmatrix}$  with

$$\mathbf{P} = \begin{pmatrix} -(\kappa + i\Delta'_c) & 0 & -iG_1 & \dots & -iG_{N-1} & -iG_N \\ 0 & -(\kappa_s + i\Delta'_s) & -iG_s & \dots & 0 & 0 \\ -iG_1^* & -iG_s^* & -(\gamma_1 + i\omega_1) & \dots & 0 & 0 \\ \vdots & \vdots & \vdots & \ddots & \vdots & \vdots \\ -iG_{N-1}^* & 0 & 0 & \dots & -(\gamma_{N-1} + i\omega_{N-1}) & -i\eta_{N-1} \\ -iG_N^* & 0 & 0 & \dots & -i\eta_{N-1} & -(\gamma_N + i\omega_N) \end{pmatrix}, \tag{S44}$$

and

$$\mathbf{R} = \begin{pmatrix} 0 & 0 & -iG_1 & \dots & -iG_{N-1} & -iG_N \\ 0 & 0 & -iG_s & \dots & 0 & 0 \\ -iG_1 & -iG_s & 0 & \dots & 0 & 0 \\ \vdots & \vdots & \vdots & \ddots & \vdots & \vdots \\ -iG_{N-1} & 0 & 0 & \dots & 0 & 0 \\ -iG_N & 0 & 0 & \dots & 0 & 0 \end{pmatrix}. \tag{S45}$$

The formal solution of the linearized quantum Langevin equations Eq. (S41) can be obtained as

$$\tilde{\mathbf{u}}(t) = \tilde{\mathbf{M}}(t)\tilde{\mathbf{u}}(0) + \int_0^t \tilde{\mathbf{M}}(t-s)\tilde{\mathbf{N}}(s)ds, \tag{S46}$$

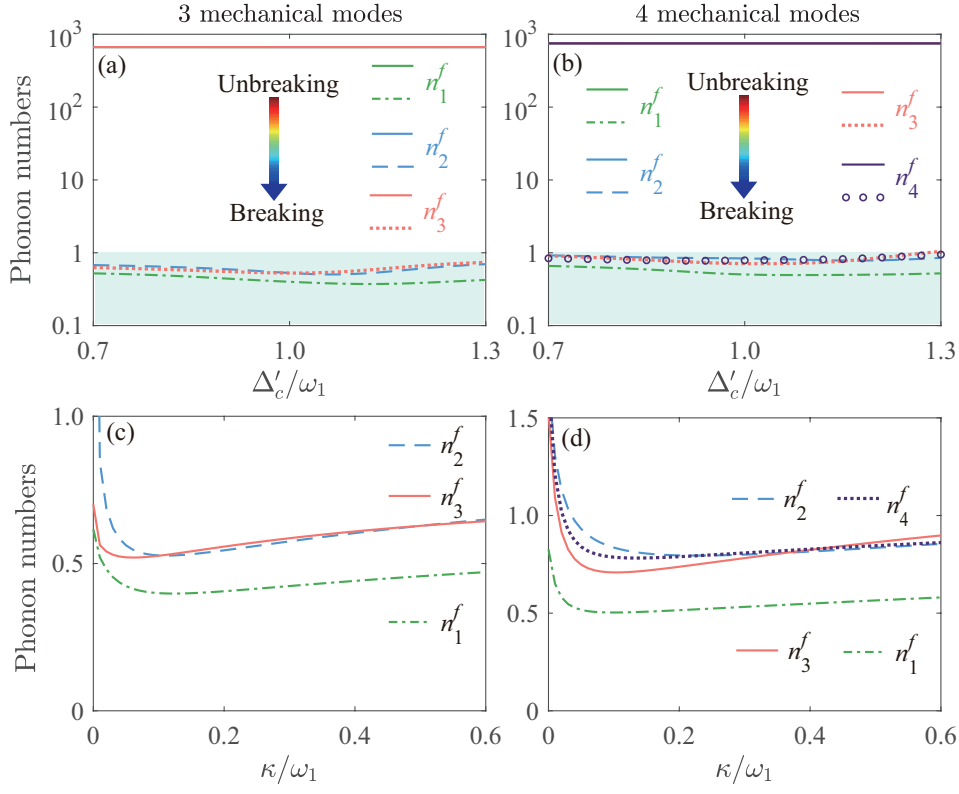


FIG. S9: The final mean phonon numbers (a) [(b)]  $n_i^f$  in these mechanical modes as functions of the effective driving detuning  $\Delta'_c/\omega_1$  in either the dark-mode-unbreaking case  $G_s/\omega_1 = 0$  and  $\eta_l/\omega_1 = 0$  or the dark-mode-breaking case  $G_s/\omega_1 = 0.1$  and  $\eta_l/\omega_1 = 0.06$  for  $N = 3$  ( $N = 4$ ). The final mean phonon numbers (c) [(d)]  $n_i^f$  in these mechanical modes as functions of the cavity-field decay rate  $\kappa/\omega_1$  for  $N = 3$  ( $N = 4$ ). The parameter  $\kappa/\omega_1 = 0.1$  is used in panels (a) and (b), the parameter  $\Delta'_c/\omega_1 = 1$  is used in panels (c) and (d). Other parameters used are  $\omega_l/\omega_1 = 1$ ,  $\Delta'_s/\omega_1 = 1$ ,  $\kappa_s/\omega_1 = 0.1$ ,  $\eta_l/\omega_1 = 0.06$ ,  $\gamma_l/\omega_1 = 10^{-5}$ ,  $G_l/\omega_1 = 0.05$ ,  $G_s/\omega_1 = 0.1$ , and  $\bar{n}_l = 1000$ .

where the matrix  $\tilde{\mathbf{M}}(t)$  is given by  $\tilde{\mathbf{M}}(t) = \exp(\tilde{\mathbf{A}}t)$ . Note that our simulations must satisfy the stability conditions derived from the Routh-Hurwitz criterion, i.e., the real part of the eigenvalues of the coefficient matrix  $\tilde{\mathbf{A}}$  is negative.

For studying the quantum cooling of these mechanical modes, we calculate the steady-state mean phonon numbers in these mechanical modes. This can be realized by calculating the steady-state values of the covariance matrix  $\tilde{\mathbf{V}}$ , which is defined by the matrix elements

$$\tilde{\mathbf{V}}_{ij} = \frac{1}{2} [\langle \tilde{\mathbf{u}}_i(\infty) \tilde{\mathbf{u}}_j(\infty) \rangle + \langle \tilde{\mathbf{u}}_j(\infty) \tilde{\mathbf{u}}_i(\infty) \rangle]. \quad (\text{S47})$$

In the linearized optomechanical system, the covariance matrix  $\tilde{\mathbf{V}}$  satisfies the Lyapunov equation

$$\tilde{\mathbf{A}}\tilde{\mathbf{V}} + \tilde{\mathbf{V}}\tilde{\mathbf{A}}^T = -\tilde{\mathbf{Q}}, \quad (\text{S48})$$

where

$$\tilde{\mathbf{Q}} = \frac{1}{2}(\tilde{\mathbf{C}} + \tilde{\mathbf{C}}^T). \quad (\text{S49})$$

Here  $\tilde{\mathbf{C}}$  is the noise correlation matrix which is defined by the elements

$$\langle \tilde{\mathbf{N}}_k(s) \tilde{\mathbf{N}}_l(s') \rangle = \tilde{\mathbf{C}}_{k,l} \delta(s - s'). \quad (\text{S50})$$

For the Markovian baths considered in this work, we have  $\tilde{\mathbf{C}}(s, s') = \tilde{\mathbf{C}}\delta(s - s')$ , where the constant matrix  $\tilde{\mathbf{C}}$  is given by

$$\tilde{\mathbf{C}} = \begin{pmatrix} 0 & 0 & 0 & \cdots & 0 & 0 & 2\kappa & 0 & 0 & \cdots & 0 & 0 \\ 0 & 0 & 0 & \cdots & 0 & 0 & 0 & 2\kappa_s & 0 & \cdots & 0 & 0 \\ 0 & 0 & 0 & \cdots & 0 & 0 & 0 & 0 & 2\gamma_1(\bar{n}_1 + 1) & \cdots & 0 & 0 \\ \vdots & \vdots & \vdots & \ddots & \vdots & \vdots & \vdots & \vdots & \vdots & \ddots & \vdots & \vdots \\ 0 & 0 & 0 & \cdots & 0 & 0 & 0 & 0 & 0 & \cdots & 2\gamma_{N-1}(\bar{n}_{N-1} + 1) & 0 \\ 0 & 0 & 0 & \cdots & 0 & 0 & 0 & 0 & 0 & \cdots & 0 & 2\gamma_N(\bar{n}_N + 1) \\ 0 & 0 & 0 & \cdots & 0 & 0 & 0 & 0 & 0 & \cdots & 0 & 0 \\ 0 & 0 & 0 & \cdots & 0 & 0 & 0 & 0 & 0 & \cdots & 0 & 0 \\ 0 & 0 & 2\gamma_1\bar{n}_1 & \cdots & 0 & 0 & 0 & 0 & 0 & \cdots & 0 & 0 \\ \vdots & \vdots & \vdots & \ddots & \vdots & \vdots & \vdots & \vdots & \vdots & \ddots & \vdots & \vdots \\ 0 & 0 & 0 & \cdots & 2\gamma_{N-1}\bar{n}_{N-1} & 0 & 0 & 0 & 0 & \cdots & 0 & 0 \\ 0 & 0 & 0 & \cdots & 0 & 2\gamma_N\bar{n}_N & 0 & 0 & 0 & \cdots & 0 & 0 \end{pmatrix}, \quad (\text{S51})$$

Based on the covariance matrix  $\tilde{\mathbf{V}}$ , the final average phonon number in the  $l$ th mechanical mode can be derived as

$$\langle \delta b_l^\dagger \delta b_l \rangle = \tilde{\mathbf{V}}_{N+l+4, l+2} - \frac{1}{2}, \quad (\text{S52})$$

where  $\tilde{\mathbf{V}}_{N+l+4, l+2}$  can be obtained by solving the Lyapunov equation.

Below we simulate the cooling performance of the mechanical modes for the cases of  $N = 3$  and 4. For convenience, we assume that all the mechanical modes have the same resonance frequencies ( $\omega_l = \omega_m$  for  $l = 1, \dots, N$ ), optomechanical coupling strengths ( $G_l = G$  for  $l = 1, \dots, N$ ), and phonon-hopping coupling strengths [ $\eta_l = \eta$  for  $l = 1, \dots, (N - 1)$ ].

In Figs. S9(a) and S9(b), we plot the final average phonon numbers  $n_l^f$  in these mechanical resonators as functions of the scaled driving detuning  $\Delta/\omega_m$  in both the dark-mode-breaking ( $G_s/\omega_1 = 0.1$  and  $\eta_l/\omega_m = 0.06$ ) and -unbreaking ( $G_s = \eta_l = 0$ ) cases. The results show that the ground-state cooling is unfeasible for these mechanical modes when the auxiliary cavity mode and phonon-hopping interactions are absent ( $G_s = \eta_l = 0$ ) [the upper curves in Figs. S9(a) and S9(b)]. This is because the phonon excitation energy stored in the dark modes cannot be extracted through the optomechanical-cooling channel.

When the auxiliary cavity mode and the couplings among these mechanical modes are introduced, a new cooling channel is formed and the dark modes are broken, then the ground-state cooling of multiple mechanical modes can be realized, as shown in Figs. S9(a) and S9(b). In Figs. S9(c) and S9(d), we plot the final mean phonon numbers  $n_l^f$  as functions of the cavity-field decay rate  $\kappa/\omega_1$ . We find that the cooling performance of the first mechanical mode is the best, because it is directly connected to the auxiliary cavity mode. The cooling performance of other mechanical modes is almost the same, because all the other mechanical modes have similar coupling connections with the cooling baths.

## B. The physical mechanism for breaking the dark modes

For studying the quantum cooling of these mechanical modes, we focus on the beam-splitting-type interactions (i.e., the rotating-wave interaction term) between these bosonic modes because these terms dominate the linearized couplings in this system, and hence we can simplify the Hamiltonian of the system by making the RWA. The linearized optomechanical Hamiltonian under the RWA is given by

$$\begin{aligned} H_I = & \Delta'_c \delta a^\dagger \delta a + \Delta'_s \delta a_s^\dagger \delta a_s + \sum_{l=1}^N \omega_l \delta b_l^\dagger \delta b_l + \sum_{l=1}^N G_l (\delta a^\dagger \delta b_l + \delta b_l^\dagger \delta a) \\ & + \sum_{l=1}^{N-1} [\eta_l (\delta b_l \delta b_{l+1}^\dagger + \delta b_{l+1} \delta b_l^\dagger)] + G_s (\delta a_s^\dagger \delta b_1 + \delta b_1^\dagger \delta a_s). \end{aligned} \quad (\text{S53})$$

To clearly see the dark-mode effect in this multiple-mechanical-mode optomechanical system, we first consider the case where the auxiliary cavity and the interaction Hamiltonians between the neighboring mechanical modes are absent, i.e.,  $\Delta'_s = 0$ ,  $\eta_l = 0$ , and  $G_s = 0$  [see Fig. S8(a)], then Hamiltonian (S53) becomes

$$H'_I = \Delta'_c \delta a^\dagger \delta a + \sum_{l=1}^N \omega_l \delta b_l^\dagger \delta b_l + \sum_{l=1}^N G_l (\delta a^\dagger \delta b_l + \delta b_l^\dagger \delta a). \quad (\text{S54})$$

For convenience, we assume that all the mechanical modes have the same resonance frequencies ( $\omega_l = \omega_m$ ) and optomechanical-coupling strengths ( $G_l = G$ ). In this case, there exists a bright mode  $B_+ = \sum_{l=1}^N \delta b_l / \sqrt{N}$  and  $(N - 1)$  dark modes which decouple

from the cavity-field mode. As a result, the phonons stored in these dark modes cannot be extracted through the optomechanical cooling channel, and then these mechanical modes cannot be cooled to their quantum ground states.

To break the dark-mode effect and realize the simultaneous ground-state cooling in the  $N$ -mechanical-mode optomechanical system, we introduce an auxiliary cavity mode optomechanically coupled to the mechanical mode  $b_1$  and phonon-hopping interaction between the neighboring mechanical modes, as shown in Fig. S8(b). Without loss of generality, we assume that all the coupling strengths of the phonon-hopping interactions are same  $\eta_l = \eta$ . Thus, we can diagonalize the Hamiltonian of these coupled mechanical modes as

$$H_{\text{mph}} = \omega_m \sum_{l=1}^N \delta b_l^\dagger \delta b_l + \eta \sum_{l=1}^{N-1} (\delta b_l \delta b_{l+1}^\dagger + \delta b_{l+1} \delta b_l^\dagger) = \sum_{k=1}^N \Omega_k B_k^\dagger B_k, \quad (\text{S55})$$

where  $B_k$  is the  $k$ th mechanical normal mode with the resonance frequency  $\Omega_k$ , and which is defined by

$$\Omega_k = \omega_m + 2\eta \cos\left(\frac{k\pi}{N+1}\right), \quad k = 1, 2, 3, \dots, N. \quad (\text{S56})$$

The relationship between the mechanical modes  $\delta b_l$  and the normal modes  $B_k$  is given by

$$\delta b_l = \frac{1}{D} \sum_{k=1}^N \sin\left(\frac{lk\pi}{N+1}\right) B_k, \quad (\text{S57})$$

with  $D = \sqrt{(N+1)/2}$ . When the auxiliary cavity does not exist, then the Hamiltonian in Eq. (S53) can be rewritten with these mechanical normal modes as

$$H_I = \Delta'_c \delta a^\dagger \delta a + \sum_{k=1}^N \Omega_k B_k^\dagger B_k + H_{\text{oi}}, \quad (\text{S58})$$

where the optomechanical-interaction Hamiltonian  $H_{\text{oi}}$  reads

$$H_{\text{oi}} = \sum_{k=1}^N \left[ \frac{G}{D} \sum_{l=1}^N \sin\left(\frac{lk\pi}{N+1}\right) \delta a B_k^\dagger + \text{H.c.} \right]. \quad (\text{S59})$$

It can be seen from Eq. (S59) that the strength of the coupling between the cavity mode  $a$  and the normal mode  $B_k$  is determined by the coefficient  $(G/D) \left\{ \sum_{l=1}^N \sin[lk\pi/(N+1)] \right\}$ . Hence, we next analyze the dependence of this coefficient on the variables  $k$  and  $N$ .

As a special case, we first analyze the case  $N = 2$ . In this case, the system is reduced to the two-mechanical-mode optomechanical system, which has been analyzed before. When  $N = 2$ , the optomechanical interaction becomes

$$H_{\text{oi}} = \sqrt{2}G\delta a B_1^\dagger + \sqrt{2}G^* B_1 \delta a^\dagger. \quad (\text{S60})$$

It is obvious that the hybrid mechanical mode  $B_2$  becomes a dark mode, which decouples from both the cavity mode  $a$  and the hybrid mechanical mode  $B_1$ , so then the ground-state cooling of the two mechanical modes becomes inaccessible.

For the case of  $N \geq 3$ , the coupling coefficient between the cavity mode  $a$  and the  $k$ th normal mode  $B_k$  in Eq. (S59) is given by  $\frac{G}{D} \sum_{l=1}^N \sin\left(\frac{lk\pi}{N+1}\right)$ . Since the form of the coupling coefficients are different when  $N$  is an odd number or an even number, below we will analyze two cases corresponding to odd and even numbers  $N$ , respectively. (i) When  $N$  is an odd number, the form of the coupling coefficient depends on  $k$ . If  $k$  is an odd number, we have  $\frac{G}{D} \sum_{l=1}^N \sin\left(\frac{lk\pi}{N+1}\right) \neq 0$ . If  $k$  is even, we have  $\frac{G}{D} \sum_{l=1}^N \sin\left(\frac{lk\pi}{N+1}\right) = 0$ . (ii) For an even  $N$ , when  $k$  is an odd number, we have  $\frac{G}{D} \sum_{l=1}^N \sin\left(\frac{lk\pi}{N+1}\right) \neq 0$ . When  $k$  is an even number, we have  $\frac{G}{D} \sum_{l=1}^N \sin\left(\frac{lk\pi}{N+1}\right) = 0$ .

Based on the above discussions, we can see that for an odd  $k$ , the coupling strength between the cavity mode  $a$  and the  $k$ th normal mode  $B_k$  is nonzero. However, for an even  $k$ , the coupling strength between the cavity mode  $a$  and the  $k$ th normal mode  $B_k$  is zero. In this case, all the even normal modes are decoupled from the cavity mode. Then ground-state cooling cannot be realized in this system due to the dark-mode effect. Nevertheless, we can introduce an auxiliary cavity mode  $a_s$  to break the dark-mode effect, which is coupled to the mechanical mode  $b_1$  via the radiation-pressure interaction. By substituting the mechanical normal modes  $B_k$  into the optomechanical Hamiltonian  $H_{\text{som}} = G_s(\delta a_s^\dagger \delta b_1 + \delta b_1^\dagger \delta a_s)$ , we can get

$$H_{\text{som}} = G_s \sum_{k=1}^N \left[ \sin\left(\frac{k\pi}{N+1}\right) \delta a_s^\dagger B_k + \text{H.c.} \right]. \quad (\text{S61})$$

It can be seen from Eq. (S61) that all the mechanical normal modes  $B_k$  are coupled with the auxiliary cavity mode  $a_s$ . If the even normal modes are decoupled from the cavity field  $a$ , the ground-state cooling of the  $N$  mechanical resonators becomes accessible through the cooling channel associated with auxiliary cavity mode  $a_s$ .